SMHI

No. 84, Jan 1999

Reports Meteorology and Climatology

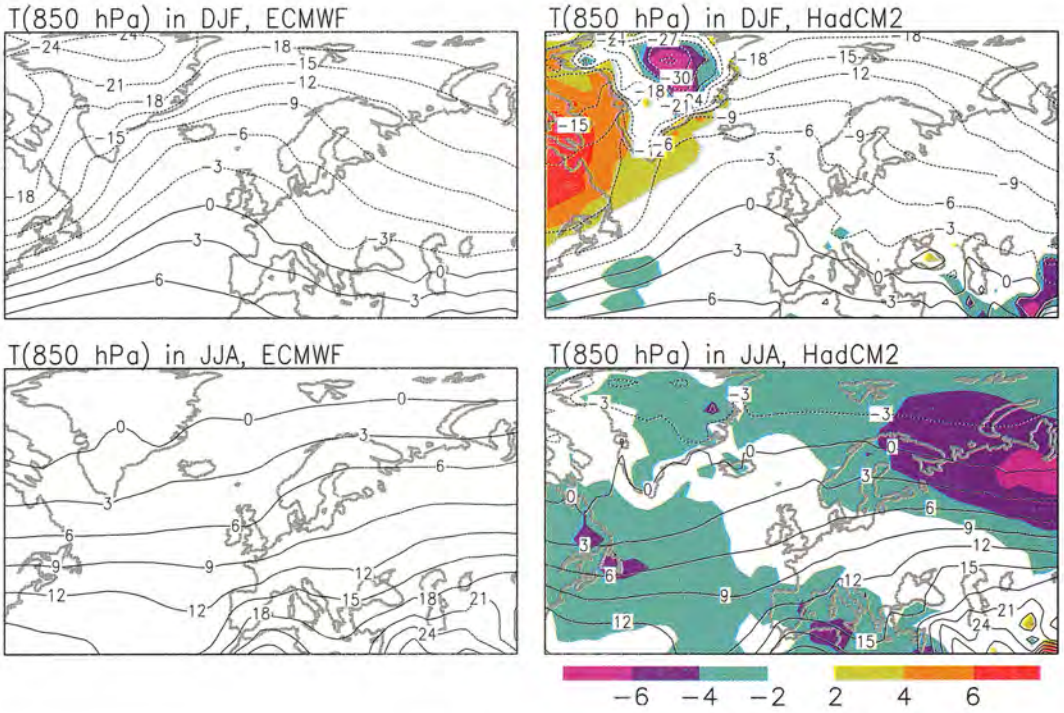

Simulation of present-day climate in Northern Europe in the HadCM2 OAGCM

Jouni Räisänen and Ralf Döscher
Rossby Centre, SMHI

Cover illustration: Seasonal mean temperatures (°C) in the lower troposphere, at the 850 hPa isobaric level, in winter (above) and in summer (below). Temperatures obtained from ECMWF analyses for 1979-1989 are shown on the left and temperatures simulated by HadCM2 on the right. The shading on the right gives the difference between HadCM2 and the ECMWF analyses.

RMK
No. 84, Jan 1999

Simulation of present-day climate in Northern Europe in the HadCM2 OAGCM

Jouni Räisänen and Ralf Döscher
Rossby Centre, SMHI

Report Summary / Rapportsammanfattning

Issuing Agency/Utgivare

Swedish Meteorological and Hydrological Institute
S-601 76 NORRKÖPING
Sweden

Report number/Publikation

RMK No. 84

Report date/Utgivningsdatum

January 1999

Author (s)/Författare

Jouni Räisänen and Ralf Döscher

Title (and Subtitle/Titel

Simulation of present-day climate in Northern Europe in the HadCM2 OAGCM

Abstract/Sammandrag

The performance of a global coupled atmosphere-ocean general circulation model, HadCM2, in simulating present-day climate in Sweden and Northern Europe is studied. The study is motivated by the use of HadCM2 within the SWEdish regional CLImate Modelling programme SWECLIM. In particular, HadCM2 provides the boundary data for the first regional high-resolution climate simulations conducted at the Rossby Centre.

HadCM2 is probably one of the best present global climate models, and several aspects of the simulated control climate are in reasonable agreement with observations. However, some quantitative shortcomings are also evident. In Northern Europe, the simulated summer temperatures are a few degrees colder than those observed, and their interannual variability appears too large. In winter, a local warm bias occurs around the Baltic Sea, which is too warm to get an ice cover in the model. The effect of the Scandinavian Mountains on the distribution of precipitation is distorted by the model's modest (2.5° lat x 3.75° lon) resolution. The simulated total cloudiness generally exceeds that observed.

In comparing the model results with the records of individual climate stations, the first problem is to derive the model-simulated value at the station location from the original discrete grid box values. Several choices of doing this are examined and, at least in comparison with observed temperature and precipitation at Swedish stations, the conclusions frequently depend on how the model-simulated station value is defined.

It is also studied how the climate in the 10-year HadCM2 control run used for dynamical downscaling at the Rossby Centre differs from a longer (240-year) control run made with the same model. In most cases, the differences between the 10-year and 240-year runs are smaller than those between the former and observations. Nevertheless, some of these differences are large enough to be kept in mind when comparing the 10-year control run with, for example, a similar run with increased CO_2.

Key words/sök-, nyckelord

Climate modelling, model evaluation

Supplementary notes/Tillägg	Number of pages/Antal sidor	Language/Språk
This work is a part of the SWECLIM programme	37	English

ISSN and title/ISSN och titel

0347-2116 SMHI Reports Meteorology Climatology

Report available from/Rapporten kan köpas från:

SMHI
S-601 76 NORRKÖPING
Sweden

Contents

1 Introduction

The activities of mankind have caused notable changes in the atmospheric composition since the preindustrial era. In particular, carbon dioxide and a number of other so-called greenhouse gases have become significantly more abundant. These gases prevent thermal radiation emitted by the Earth's surface and the warm lower atmosphere from escaping directly to space. Increases in their concentration are, therefore, expected to lead to generally higher surface temperatures. During the last century, the global mean surface air temperature has actually risen by roughly 0.5°C, which is, taking into account best estimates of other forcing factors such as sulphate aerosols and changes in solar activity, fully consistent with model results (Santer et al. 1996). More importantly, the long atmospheric lifetimes of carbon dioxide and many other greenhouse gases ensure that any realistic emission scenarios will lead to significant further increases in the concentrations of these gases in the future (e.g., Houghton et al. 1996, Technical Summary). Together with the time lag associated with the heat capacity of the world ocean, this indicates that greenhouse gas induced climate change will grow substantially larger during the next century. To help the adaptation of human activities to these changes, realistic scenarios of future climate are needed.

Much of our knowledge on the potential climatic effect of increased greenhouse gas concentrations is based on the results of three-dimensional coupled ocean-atmosphere general circulation models (OAGCMs). In the sense that these models cover the whole of the globe and describe a large number of interacting processes in the atmosphere, ocean, sea ice and land surface, OAGCMs undoubtedly are our most comprehensive tool for studying climate change. Unfortunately, however, the huge computational cost of these models presently precludes running them with a horizontal resolution higher than a few hundred kilometers. This is problematic for impact studies, which often require climatic data at considerably smaller spatial scales.

The SWEdish regional CLImate Modelling program (SWECLIM) aims to produce scenarios of future climate in the Nordic area which have a higher resolution and accuracy than presently available. This goal requires downscaling of GCM results to finer spatial scales (Giorgi and Mearns, 1991). Both dynamical (i.e, running a higher-resolution regional climate model using OAGCM-produced boundary data) and statistical downscaling (relating local-scale surface parameters to larger-scale flow) will be applied within SWECLIM. However, these interpretation techniques are only expected to be successful if the large-scale climate response is simulated realistically by the driving OAGCM.

How well a model simulates future climate changes is of course not easily determined - if we already knew the ground truth, no model experiments would be needed. However, some inferences of the potential usefulness of a model in this respect can be made by

studying how accurately the current climate is simulated. This report evaluates the simulation of present-day climate in the OAGCM used for the first SWECLIM downscaling experiments, HadCM2 (Johns et al. 1997). The motivation is on the one hand to get an impression of the adequacy of this OAGCM in providing input data for dynamical and statistical downscaling, on the other hand to get a benchmark against which to compare the results of these interpretation methods.

2 The HadCM2 OAGCM

The coupled ocean-atmosphere general circulation model HadCM2 is described in some detail by Johns (1996) and Johns et al. (1997). HadCM2 is a 'state-of-the-art' OAGCM with a horizontal resolution of 2.5°deg in latitude × 3.75°deg in longitude, or 280 x 210 km at 60°N. It includes fully dynamic three-dimensional model components for both the atmosphere and the ocean, with parametrical representation for several subgridscale physical processes. Various thermodynamical and hydrological processes occurring at the land surface and the development and movement of sea ice are also modelled. Technical characteristics of the model are summarized in Table 1. From the last row one may note that the estimated climate sensitivity of the model (i.e., equilibrium change in global mean surface air temperature in response to doubling of atmospheric CO_2) exactly coincides with the central estimate of the IPCC, 2.5°C.

Table 1. *Characteristics of the HadCM2 climate model. SW denotes short-wave (solar) and LW long-wave (terrestrial) radiation.*

Atmospheric resolution	2.5°lat × 3.75°lon; 19 hybrid levels
Ocean resolution	2.5°lat × 3.75°lon; 20 levels
Spinup	Coupled spinup for 510 years
Radiation scheme	4 bands in SW + 6 bands in LW (Slingo and Wilderspin 1986; Slingo 1989). Trace cases explicitly accounted for are H_2O, O_3 and CO_2.
Convection parameterization	Penetrative convection scheme with explicit downdraught (Gregory and Rowntree 1990; Gregory and Allen 1991)
Vertical diffusion	First-order (Smith 1990)
Surface scheme	Soil temperature predicted in 4 layers with zero heat flux at the base. Snow cover and soil water predicted. Canopy effects are taken into account. (Warrilow et al.1986)
Time integration scheme	Split-explicit (Cullen and Davies, 1991), advection with Heun (Mesinger 1981)
Time steps	30 min atmosphere; 60 min ocean
Model output	Every 6 hours
Explicit corrections during time integration	Atmospheric energy and mass loss; negative humidities
Flux corrections	Seasonal averages, calculated from 25 years of coupled spinup
Prognostic variables	Surface pressure, horizontal wind, total water mixing ratio, liquid water potential temperature
Climate sensitivity	2.5°C

A general verification of the HadCM2 'control simulation' against observational data has been conducted by Johns et al. (1997) and Tett et al. (1997). Some aspects were also studied by Räisänen (1997). An overall impression from these studies is that, although HadCM2 does have its weaknesses, it still is one of the best OAGCMs available today. This report complements the afore-mentioned global studies by investigating the ability of HadCM2 to simulate the present climate in Northern Europe.

Worth noting is that the analysis in this report is mostly based on a 10-year period (September 2039 – December 2049) in a 'repeated' control run, rather than on the much longer original control run used by Johns et al. (1997) and Tett et al. (1997). The repeated control run (or briefly rerun) was made to provide the Rossby Centre and other regional climate modelling groups with the boundary data required for driving their limited area models – the data archived from the original control run were not detailed enough for this purpose. Initial conditions for the rerun were from the beginning of September 2039 in the original control run, but a different computer was used. Because of nonlinear amplification of the initially bit-level differences, the climate of the repeated 10-year period is not identical with that during the same period in the original control run. However, the differences appear to be within the natural interdecadal variability in the original control run.

Ten years is a relatively short time slice of model-simulated climate – in particular at high latitudes where interannual and interdecadal variations of climate are large. The 10-year period is used here on one hand for practical reasons (some of the variables studied here were only available for this period) and on the other hand for the very fact that this happens to be the period used in the SWECLIM downscaling work. However, neither of these arguments removes the need for checking how characteristic the 10-year period is of the longer-term behaviour of the model. To the extent that available data allow, we will study this issue in the next-to-last section of this report by comparing the statistics for the 10-year period with those for the first 240 years (1860-2099) of the original control run. The 240-year period will also be used in studying the interannual variability of surface air temperature and precipitation (section 7), since this issue cannot be meaningfully addressed with just 10 years of data.

Noteworthy is that the atmospheric equivalent CO_2 concentration in the HadCM2 control run was held constant at the preindustrial level and the anthropogenic aerosol loading was neglected. Therefore, some of the differences between the modelled and observed climates might arise because the model strictly speaking attempts to simulate the preindustrial rather than the present climate. As noted by Räisänen (1997), however, the overall relative importance of this factor for the model-observation differences is expected to be small.

The main focus of this report is on the time mean surface climate: monthly and seasonal means of surface air temperature, precipitation, and to a lesser extent total cloudiness

(sections 5 and 6). However, we will also discuss the atmospheric circulation near the surface and in the free atmosphere including variability at synoptic time scales (section 3), the modelled sea surface temperatures (section 4), and the interannual variability of surface climate (section 7). Finally, after the mentioned comparison between the 10-year and 240-year control runs (section 8), the main findings are summarized in section 9.

3 Atmospheric circulation

The ability of HadCM2 to simulate the atmospheric circulation over Europe and the North Atlantic ocean is studied in this section by using four variables. Three of these (sea level pressure, 850 hPa temperature and 300 hPa zonal wind) characterize the time-mean climate near the surface and in the free troposphere. The last variable, high-pass filtered transient kinetic energy at 850 hPa, is a measure of lower tropospheric baroclinic activity. The filtering follows Hoskins et al. (1989) and retains 90% (75/ 50/ 25/10%) of the total variance when the period of the fluctuation is 4.0 d (4.9/6.7/10.2/16.6 d). In Figs. 3.1 and 3.2, the HadCM2 simulated winter (December-February; DJF) and summer (June-August; JJA) climate during 2039-2049 is compared with observational estimates from the Hoskins et al. (1989) compilation of the ECMWF (European Centre for Medium Range Weather Forecasts) analyses for 1979-1989.

The observed time-mean sea level pressure field in winter (Fig. 3.1a) is dominated by a deep Icelandic low, with increasing pressure towards lower midlatitudes and Siberia. HadCM2 reproduces this basic pattern, but in northern Europe the northwest-southeast pressure gradient is underestimated. This feature mainly results from a shallower than observed northeastward extension of the Icelandic low toward the Arctic Ocean, and it indicates that the time-mean near-surface souhwesterly flow is somewhat too weak in the model. Noteworthy is that, as a result of purely numerical leakege of mass (Johns 1996), the global mean sea level pressure in HadCM2 is about 3 hPa too low. Because absolute values of sea level pressure are of lesser importance than pressure differences, a direct comparison between the numbers in Figs. 3.1a-b and 3.2a-b is slightly misleading. To help the interpretation, the colour scale indicating the differences between the model and the observations is in these figures uncentered by 3 hPa.

In summer (Figs. 3.2a-b), the observed pressure pattern is flatter than in winter and is dominated by a high over the subtropical North Atlantic and decreasing pressure towards the Asian monsoon low in the southeast. The basic features are very similar in HadCM2. The pressure decrease towards the Asian monsoon low is somewhat too sharp, but this impression may be partly caused by differences in estimating sea level pressure in mountain areas.

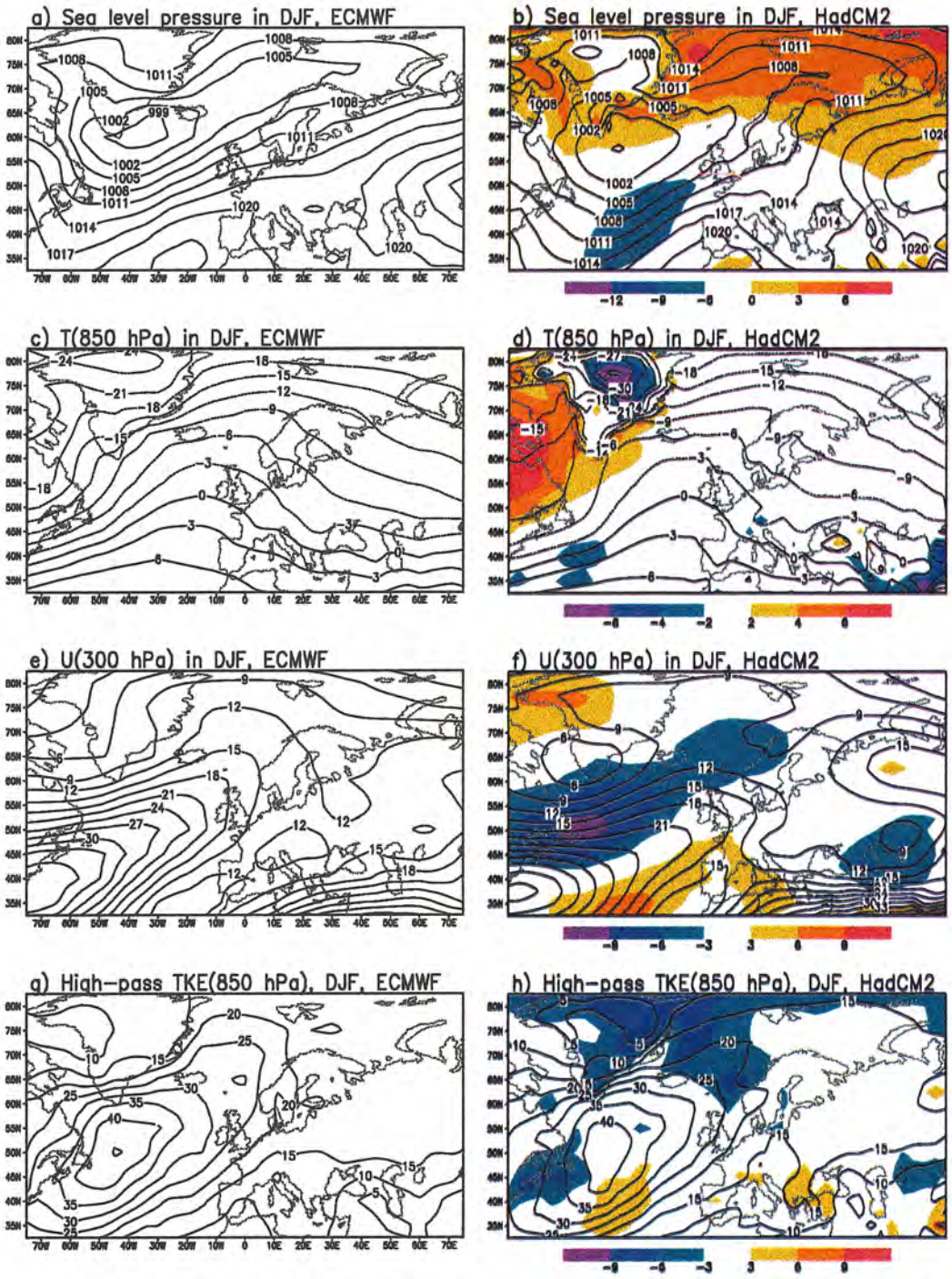

Figure 3.1: *Observational estimates (left; Hoskins et al. 1989) and HadCM2 simulation results (right) for four variables during the northern winter (December-February). (a)-(b) sea level pressure (contours every 3 hPa), (c)-(d) temperature at 850 hPa (every 3°C), (e)-(f) zonal wind component at 300 hPa (every 3 m/s) and (g)-(h) high-pass filtered transient kinetic energy at 850 hPa (every 5 m^2s^{-2}). The difference between HadCM2 and the observational estimates is indicated by the colour scale in the right-hand-side panels. The colour scale in (b) is uncentered by 3 hPa to take into account the difference in global mean sea level pressure (see text).*

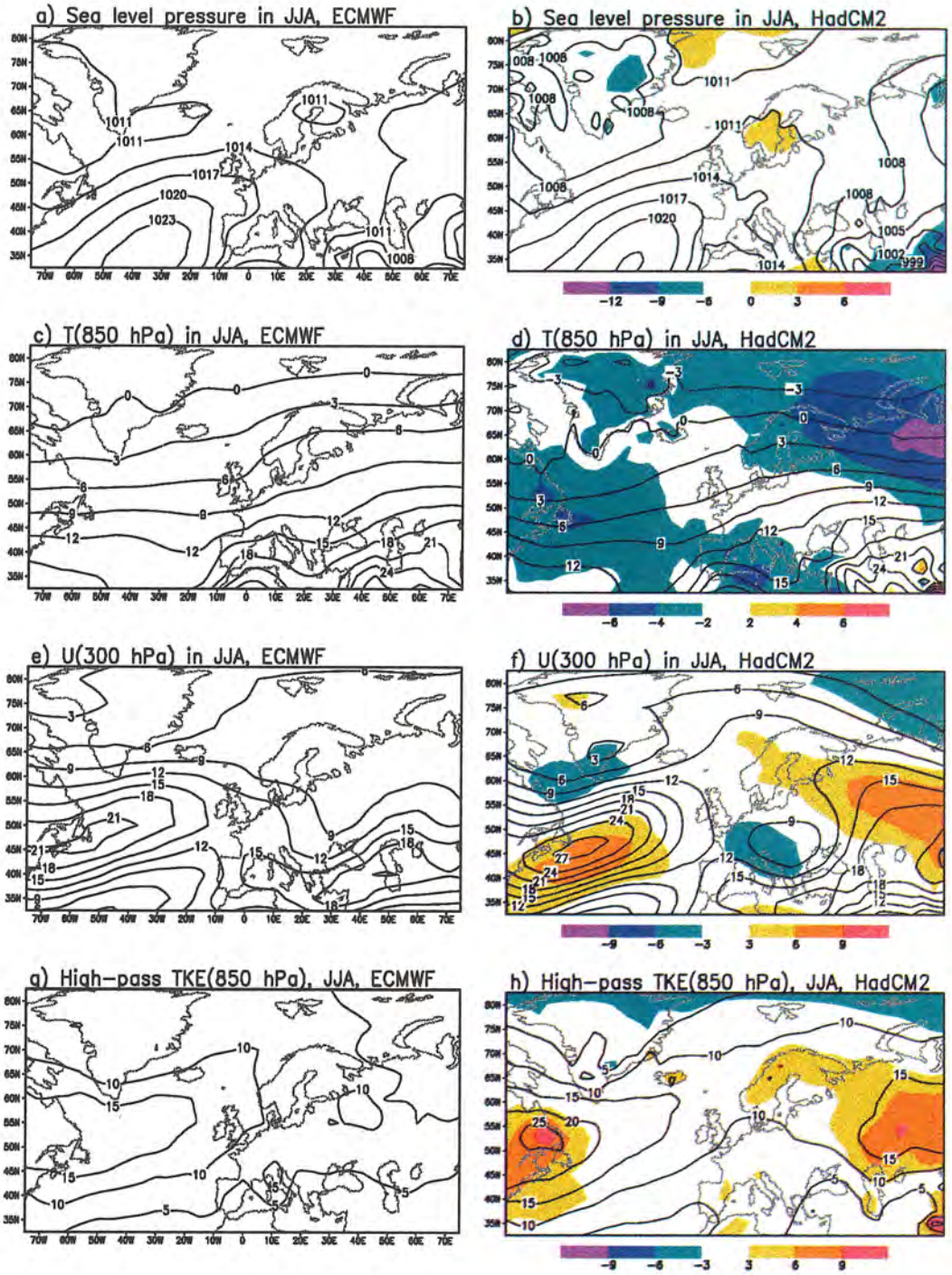

***Figure 3.2**: As Fig. 3.1, but for summer (June-August)*

Although there are some differences from the observed climate, the model-simulated distribution of sea level pressure in the Atlantic-European area is as whole very reasonable in both winter and summer. This is also the case in other regions of the world: Räisänen (1997) found a global spatial correlation of 0.96 between the simulated and observed pressure distributions in both DJF and JJA.

The wintertime 850 hPa temperatures in HadCM2 are, over much of Europe and the northern North Atlantic, relatively close to those observed (see Figs. 3.1c-d). A slight cold bias occurs at lower midlatitudes, but in northeastern North America the HadCM2 simulation is up to 8°C warmer than the observed climate. Hence, the lower tropospheric baroclinicity at the east coast of North America is too weak and concentrated too far south. The apparent cold bias in HadCM2 over high topography in Greenland may be an artefact associated with below-ground temperature extrapolation.

In summer (Figs. 3.2c-d), there is a rather widespread cold bias in HadCM2. Over the Nordic countries, for example, this bias is 2-4°C. In eastern Europe and western Siberia, the bias increases towards north and the meridional temperature gradient is overestimated.

Globally, the HadCM2 simulated temperatures tend to be somewhat too cold in both seasons, not only in the lower troposphere but also at upper levels. The zonal mean cross sections shown by Johns et al. (1997) reveal a cold bias in of 1-2°C in most of the middle and lower troposphere, and a substantially larger cold bias at the tropopause level in the tropics and near the summer pole. In the lower troposphere north of 45°N, however, there is a warm zonal mean bias of 1-3°C in the northern winter.

The time mean zonal wind component at 300 hPa in winter is shown in Figs. 3.1e-f. The maximum of the north Atlantic jet stream at the east coast of North America is in fact marginally stronger in HadCM2 than according to the observational data, but the simulated jet stream is slightly too far south. Therefore, the zonal wind further north over the Atlantic is underestimated in the model. In summer (Figs. 3.2e-f), the core of the Atlantic jet is significantly too strong in HadCM2, but even in this season the simulated wind maximum is slightly too south. Consistent with the stronger than observed meridional temperature gradient, the model also simulates somewhat too strong zonal winds in a belt extending from Scandinavia towards inner Russia.

The lowermost panels in Figs. 3.1 and 3.2 compare the high-pass filtered transient kinetic energy at 850 hPa in HadCM2 and according to the ECMWF analyses. The wintertime maximum to the east of Newfoundland is well located and nearly of the right magnitude. Over the Norwegian sea and the Arctic Ocean, the simulated activity is somewhat weaker than observed, consistent with the too shallow pressure trough in this area. The simulated activity is also too low over the Arctic in summer. In this season, however, the maximum over eastern Canada and western North Atlantic is somewhat too strong in the model. The activity is also somewhat too high over northern and eastern Europe, where the meridional temperature gradient is overestimated.

Johns et al. (1997) study the synoptic variability in HadCM2 by using a band-pass (2-6 day frequency band) filtered variance of the 500 hPa height field. They find the Atlantic storm track to be somewhat too south and, in particular in its eastern part, slightly too

weak in both winter and summer. These features are not all revealed in our study of the 850 hPa kinetic energy (which, in particular, indicates a slightly overestimated rather than underestimated transient activity in summer), but there are several sources of difference. Apart from using a different variable (high-pass filtered kinetic energy vs. band-pass filtered height variance) we also use a different time period (years 2039-2049 in the repeated control run vs. 1860-1989 in the original control run) and a different vertical level. In the midtroposphere, the high-pass filtered kinetic energy is actually similar in magnitude to that observed in JJA, and distinctly below that observed in DJF. Moreover, the relatively southerly position of the maximum activity is more apparent in the upper and midtroposphere than at 850 hPa.

4 Sea surface temperatures in the North Atlantic Ocean

Coupled climate models like HadCM2 contain, in addition to an atmospheric GCM, an oceanic GCM of similar complexity. To illustrate the performance of the HadCM2 ocean model, the simulated sea-surface temperatures (SSTs) in the North Atlantic Ocean are briefly discussed in this section. Some further remarks on the model behaviour in the Baltic Sea will be given later.

The HadCM2 10-year mean SST climatology is compared to the World Ocean Atlas 1994 (Levitus and Boyer 1994), which is the most comprehensive compilation of present-day ocean temperatures. Figs. 4.1a and 4.1b show the annual means of observations and HadCM2. The difference is given in Fig. 4.1c: the HadCM2 simulation is colder than the observations in the southwestern North Atlantic and warmer in the northeastern North Atlantic. The Norwegian Sea also has warmer SSTs in HadCM2. Maxima of up to 2 K in the annual mean model-observation difference occur at two locations above the Northatlantic sill between Greenland and Iceland and in the triangle between Iceland, Scotland and Norway. The annual cycle is indicated by Figs. 4.1d – 4.1g. The Iceland-Scotland-Norway warm bias in HadCM2 is strongest in winter and weak in summer. The Greenland-Iceland maximum nearly persists in amplitude, but is reduced in area during summer. The general picture of warmer than observed SST in HadCM2 off Norway is prevalent all year with minor intrusions of colder SST in winter and spring.

The reason for these deviations can be found in the general circulation structure of the OGCM and in deficiencies modelling local processes. The North Atlantic Current (NAC) is too weak and broad in the coarse resolution HadCM2 ocean. This is associated with a weak heat transport leading to SSTs lower than expected. The northern extension of the NAC lacks flow across the North Atlantic sills, so that the northeastern North Atlantic gets too warm. These deficiencies are partly compensated for by flux adjustments in the coupling between ocean and atmosphere. The deviations from the observed SSTs in the Nordic Seas indicate wrong mixed layer depths and local ocean convection problems.

As will be further discussed in the next section, Fig. 4.1d also shows that the grid boxes representing the northern parts of the Baltic Sea are several degrees too warm in the model in winter.

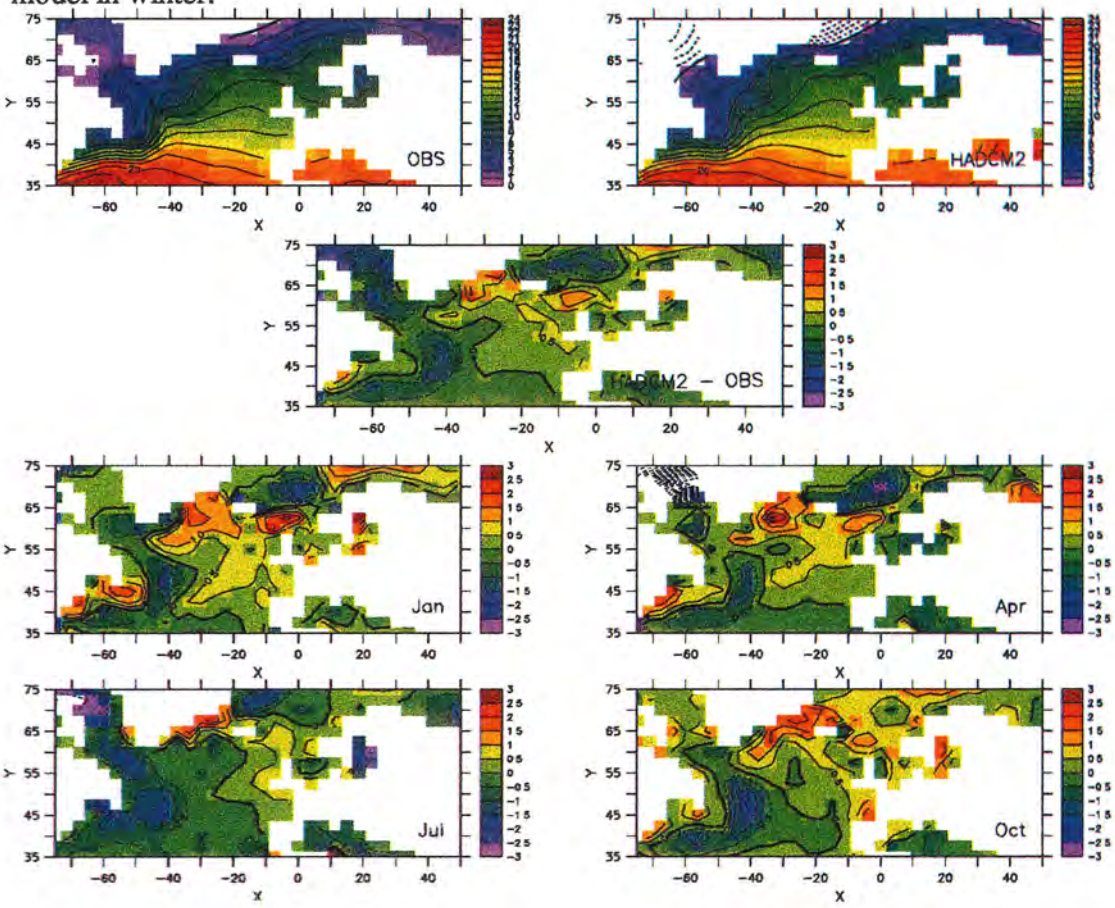

Figure 4.1: Comparison of simulated and observed sea surface temperatures (°C). Annual means: (a) observations [Levitus and Boyer 1994], (b) HadCM2 control run and (c) HadCM2 -observations. Differences between HadCM2 and observations in individual months: (d) January, (e) April, (f) July and (g) October.

5 Temporal mean surface climate: comparison with the CRU climatology

In this and the following section, the temporally averaged (seasonal and monthly means during 2039-2049) surface climate in HadCM2 is compared with two sets of observational data for the period 1961-1990. The first of these, used in this section, is the gridded land area climatology prepared by Hulme et al. (1995) at CRU (Climatic Research Unit, University of East Anglia), which has a resolution of 0.5° in both latitude and longitude. Second, in section 6, the model simulation is compared with climatological means for individual weather stations in Sweden (Alexandersson et al. 1991). The comparison with the CRU climatology includes three variables (surface air

temperature, precipitation and total cloudiness), that with the Swedish stations two (surface air temperature and precipitation).

5.1 Surface air temperature

Fig. 5.1 shows the seasonally averaged surface air temperature in northern Europe as obtained from the CRU data set and as simulated by HadCM2. Four standard three-month seasons are used: winter = December – February (DJF); spring = March – May (MAM); summer = June – August (JJA); autumn = September – November (SON).

A first obvious difference between the observations and the model results is the lack of spatial detail in the latter. With its grid size of 2.5° in latitude x 3.75° in longitude, HadCM2 only crudely resolves the Scandinavian Mountains and the Baltic and Atlantic coastlines. Hence, many regional features in the temperature distribution associated with topography and land-sea contrasts are lost.

Due to the difference in resolution, a quantitative comparison between the observations and the model simulation is somewhat complicated. In the right-hand-side panels of Fig. 5.1, such a comparison is made with the simplest approach. The observational data are regridded to the coarser HadCM2 grid, taking an area-weighted average of all available CRU grid values within each HadCM2 grid cell. As the CRU data set only includes land areas, HadCM2 sea grid boxes are excluded from the comparison although some CRU land grid boxes frequently fall within them. For simplicity, no adjustment is made for the height difference between the HadCM2 and CRU orographies. After regridding the latter to the HadCM2 grid, the two orographies are in fact relatively close to each other. The largest difference between them is 200 m (over the Scandinavian mountains, where the HadCM2 orography is lower), which implies an adjustment of only 1°C[1].

This coarse-grid comparison indicates that, in all seasons except in winter and locally in autumn, HadCM2 simulates somewhat too cold temperatures over the Nordic Countries. The cold bias is largest in northern and western parts of the Nordic area in summer, varying in Finland, northern Sweden and Norway between 2° and 4°C. However, the summertime bias is reduced towards southeast and in the eastern parts of Central Europe HadCM2 in fact simulates somewhat too warm temperatures. Both of these features, the cold bias in northern Europe and the exaggerated meridional temperature gradient, are consistent with the 850 hPa temperatures discussed in the previous section. In spring, the cold bias over the Nordic Countries is slightly smaller than in summer, but in this season the simulated temperatures are below those observed also in central and eastern Europe.

[1] The effect of such height adjustments will be studied in the next section by using vertical lapse rates of temperature assumed by the CRU data set.

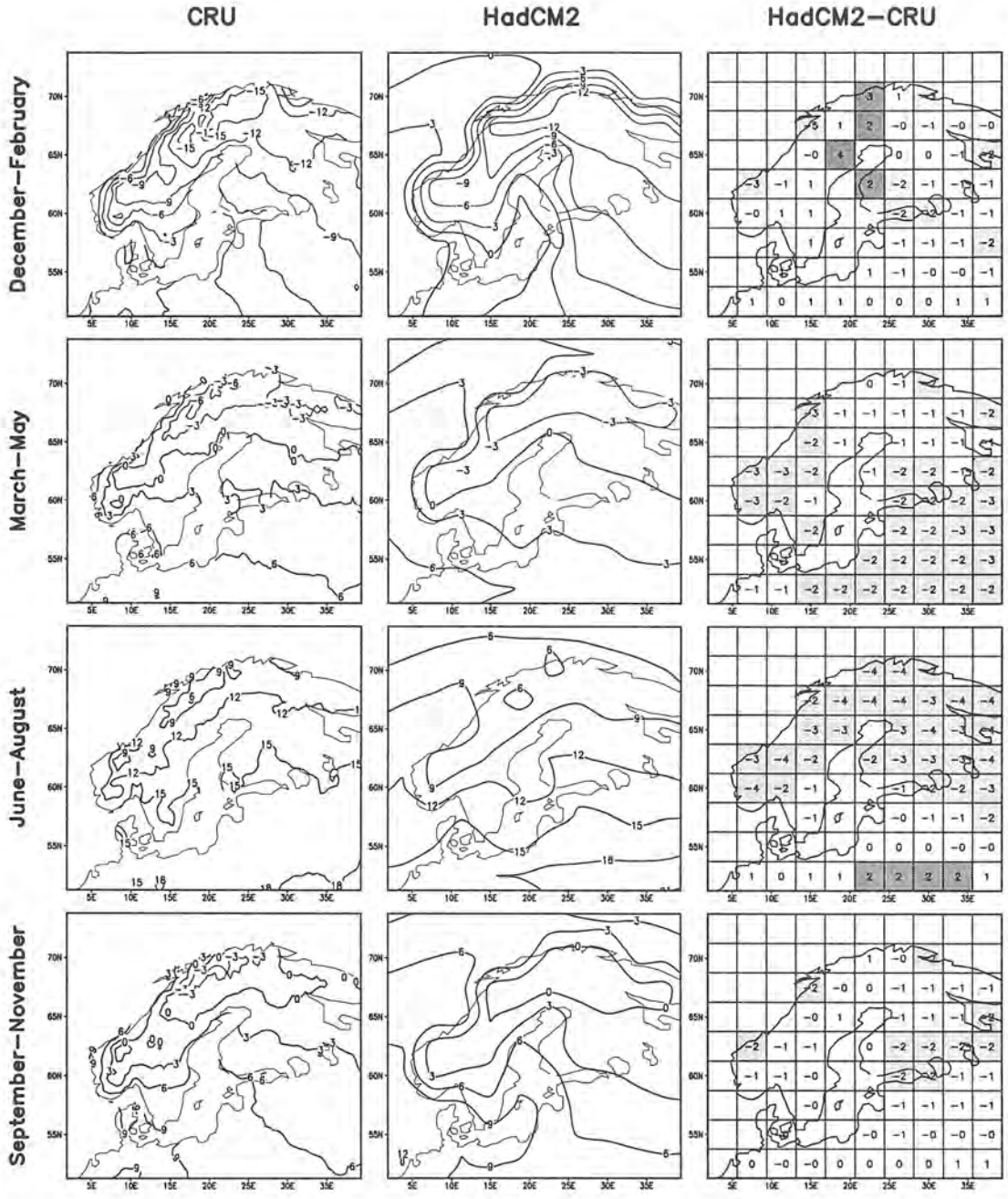

***Figure 5.1**: Seasonally averaged surface air temperatures (°C) in northern Europe. The left column shows the CRU medium-height climatology for 1961-1990 and the midcolumn temperatures in the HadCM2 repeated control run in 2039-2049. On the right, the difference between HADCM2 and CRU is shown after regridding the CRU temperatures to the HadCM2 land grid boxes. Areas where HadCM2 is more than 1.5°C warmer (colder) than observations are shaded in dark (light).*

The simulated temperatures are also slightly below those observed in most of the Nordic area in autumn. In western Scandinavia and in the eastern half of Finland this is the case even in winter. However, in the grid boxes surrounding the Baltic Sea the bias is of

varying sign in autumn and generally positive in winter, in particular around the northern parts of the basin. This regional warm bias probably stems from a poor simulation of the Baltic Sea winter conditions. As already noted in the previous section, the sea surface temperatute in the grid boxes representing Bothnian Sea and Bothnian Bay is spuriously high in winter, and even in the coldest winters the whole Baltic Sea remains ice-free (see also Fig. 5.2). This enables unrealistically large fluxes of sensible and latent heat to the atmosphere in particular in the northern parts that are usually ice-covered in nature.

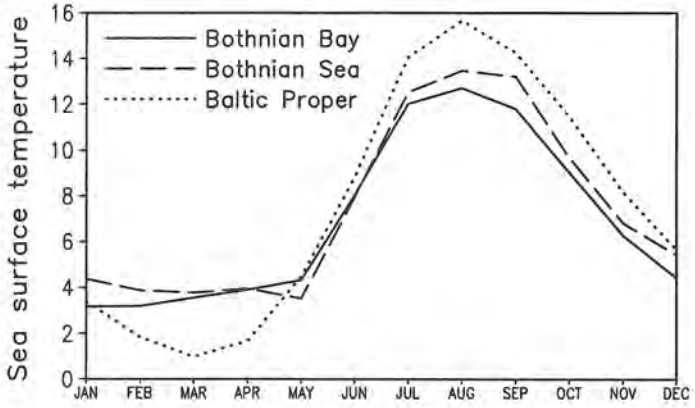

***Figure 5.2**: 10-year mean (2039-2049) seasonal cycle of sea surface temperature in HadCM2 in Bothnian Bay (65°N, 22.5°E; solid line), Bothnian Sea (62.5°N, 18.75°E; dashed line) and Baltic Proper (57.5°N, 18.75°E; dotted line).*

5.2 Precipitation

In Fig. 5.3, the precipitation in the HadCM 2 control simulation is compared with the CRU climatology. The impact of the model's modest resolution is in fact much larger than in the case of temperature. The observational data show, in all seasons but most dramatically in autumn and winter, a band of very abundant precipitation over the western slopes of the Scandinavian Mountains. In HadCM2, this maximum band is weaker and smoother and displaced to the east, rather over the top than over the western slope of the heavily rounded mountain range.

To the east of the Scandinavian Mountains, the HadCM2-simulated precipitation generally exceeds the CRU climatology in winter and spring. In some part, however, this difference is an artifact of the observational data. The CRU climatology does not include corrections for measurement errors that are known to cause a significant underestimate of, in particular, solid precipitation (e.g., Legates and Willmott 1990). In summer, by contrast, the simulated precipitation is relatively close to that observed in much of Finland and Sweden, and substantially below that observed in western Russia and in the Baltic States. In autumn, precipitation in HadCM2 again exceeds the CRU climatology in particular in northern Finland and Sweden.

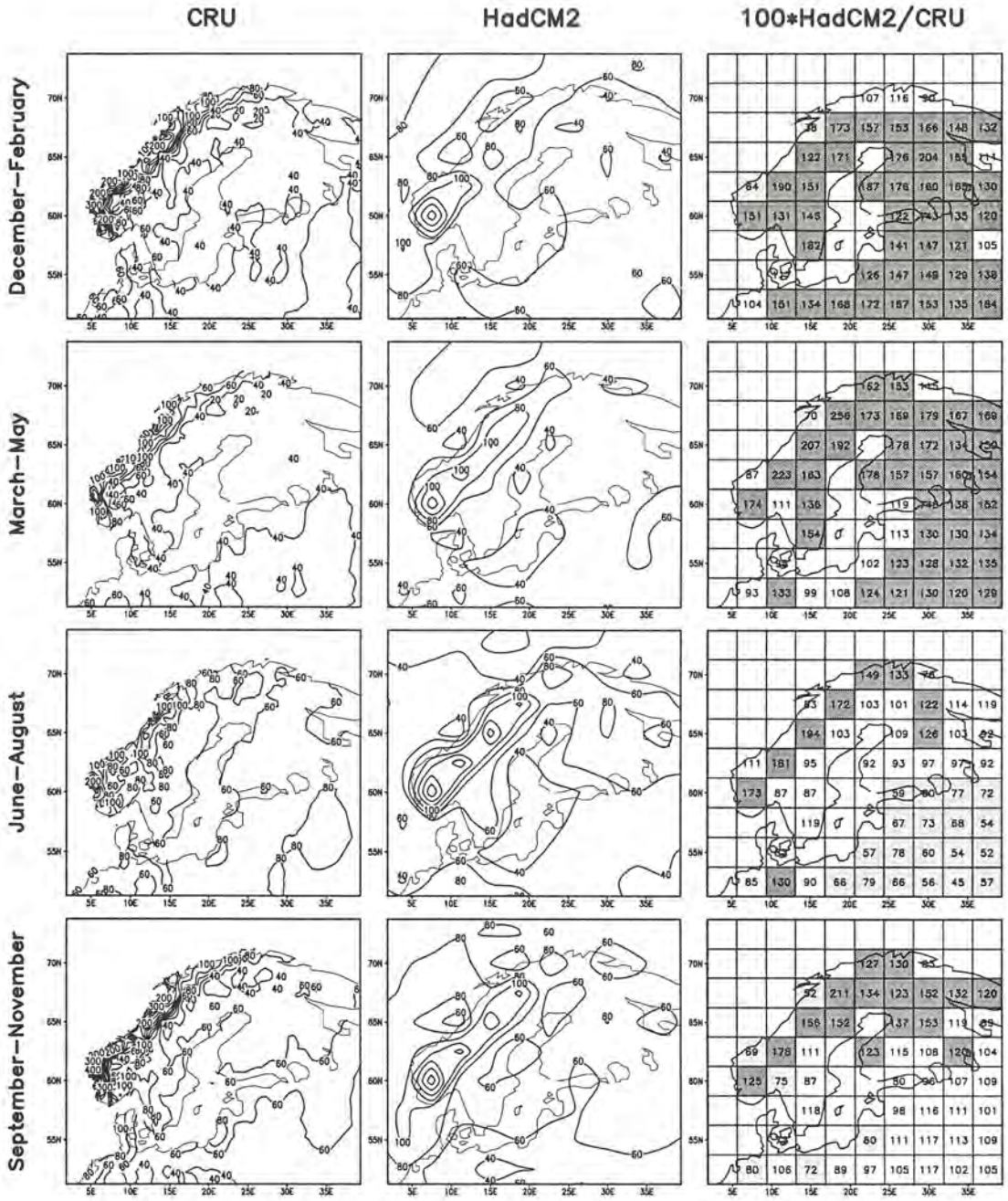

Figure 5.3: As Fig. 5.1, but for precipitation (isolines at every 20 mm/month but only 20, 40, 60, 80, 100, 200, 300 and 400 mm/month are labelled). The numeric values in the right column show the ratio between the model-simulated precipitation and the regridded CRU medium height climatology in percent. Areas in which precipitation in HadCM2 is at least 20% larger (smaller) than observed are shaded dark (light).

5.3 Total cloudiness

Finally, the HadCM2-simulated total cloudiness is compared with the CRU climatology in Fig. 5.4. As whole, the model simulates a greater cloud cover over Northern Europe than the CRU climatology indicates.

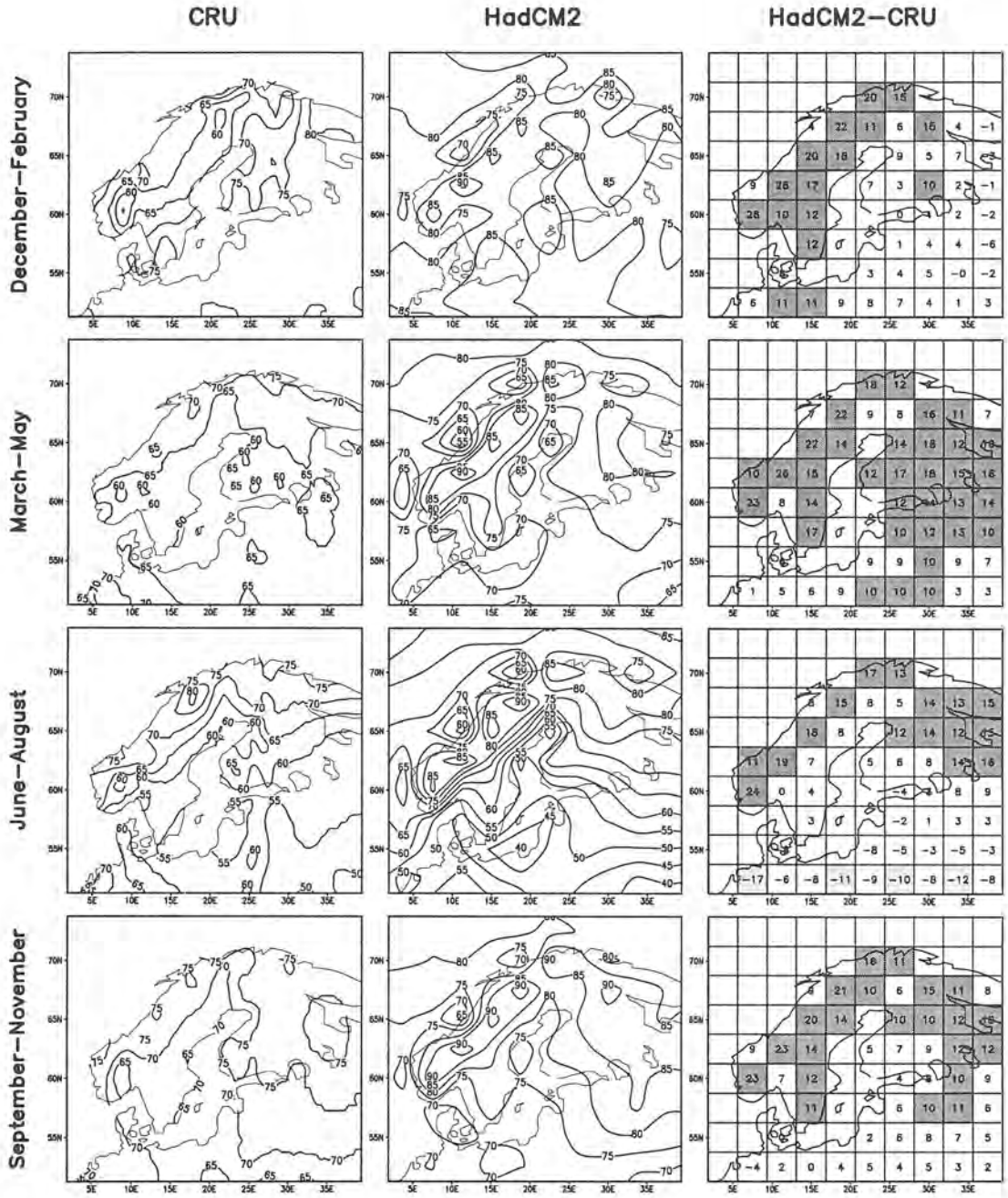

***Figure 5.4**: As Fig. 5.1, but for seasonal mean total cloudiness (per cent of full cover). In the right column, areas where the simulated cloudiness is at least 10 per cent units larger (smaller) than observed are shaded dark (light).*

Simulated total cloudiness is particularly large over the Scandinavian mountains, locally 85-90% in all seasons. Although observations also reveal a maximum of cloudiness over or at the western side of the mountain range, this is less pronounced. However, even in southern and eastern parts of Sweden, well away from the mountains, simulated cloudiness exceeds the observational estimate by at least 10% of full cover in all seasons

except in summer. In parts of Finland, the difference from observations is slightly smaller in autumn and winter, when the observed cloudiness is rather high (order of 75%) as well. The largest overestimate in Finland occurs in spring, when the model-simulated total cloudiness remains much closer to its wintertime level than the CRU climatology indicates.

Another unrealistic feature in the HadCM2 simulation is the very steep southward decrease in summertime cloud cover in particular over the western parts of the former Soviet Union. As seen from Fig. 5.1, this overly sharp gradient in cloudiness coincides with an overestimated meridional gradient in surface air temperature.

Total cloudiness is naturally not an exactly observed quantity. Some sources of error in surface observations might act to make the estimated cloud cover too small (for example, optically thin high clouds are not easily detectable at night) and thus widen the gap between observations and the model simulation. However, cloud cover estimates from the satellite-based ISCCP (International Satellite Cloud Climatology Project) D2 data set (Rossow et al. 1996) are generally much closer to the CRU climatology than the HadCM2 simulation (not shown). This suggests that the main findings of this section are not sensitive to uncertainties in observational data.

6 Comparison with Swedish meteorological stations

Many practical applications need climatic data at local scales, for example time series at individual meteorological stations. Deriving such local-scale data from GCM output is unfortunately not a trivial matter, even if the simulated large-scale climate were perfect. The most fundamental difficulty is that a GCM only predicts a set of grid box values, not a continuous distribution. As illustrated in Fig 6.1 for the case of January mean surface air temperature in HadCM2, the simulated values in adjacent grid boxes may differ considerably from each other. The simplest way of applying GCM data at local scales – assuming that each grid box value is valid in the whole grid box – therefore results in large jumps at grid box boundaries.

The discontinuity problem may be avoided by assuming that the simulated grid box values actually are a sample of some continuous physical distribution. A simple and frequently used way of doing this is bilinear interpolation. The continuous field is assumed to coincide with the simulated grid box values at grid box centers ('grid points'), and between these, the field is assumed to be a linear function of both latitude and longitude. The local value thus generally becomes a weighted average of the four nearest GCM simulated grid box values.

Another problem, which cannot be cured by a simple horizontal interpolation, are differences in physiography between GCMs and nature. For example, in mountainous areas there are often substantial small-scale variations in surface topography that are

necessarily lacking from a GCM height field. The distributions of land and water also occasionally differ between GCMs and nature, which is in some areas an even more serious problem than differences in orography. For example, as seen from Fig. 6.1, Stockholm and many other towns at the eastern coast of Sweden are actually within sea grid boxes in HadCM2.

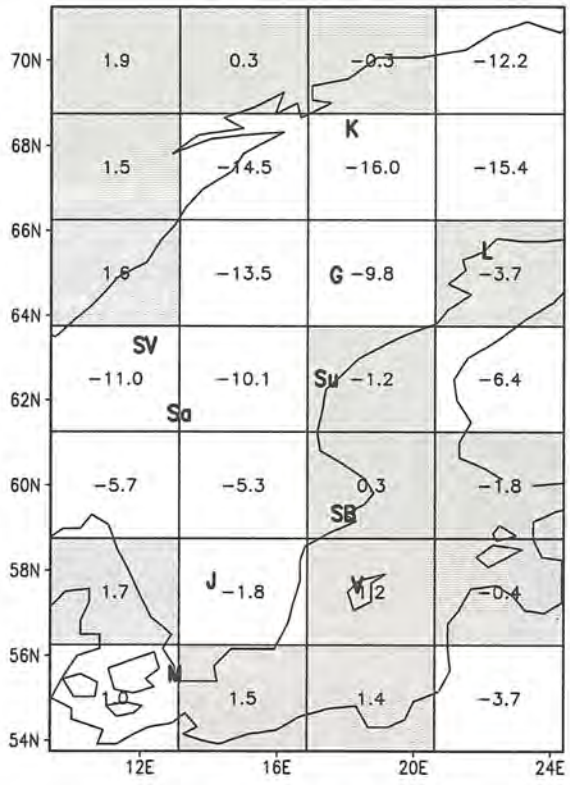

***Figure 6.1**: HadCM2-simulated January mean temperatures during 2040-2049, given as numeric values at each grid box center. The shaded grid boxes are sea in HadCM2. The letters show the locations of the ten Swedish meteorological stations used in Figs. 6.2 and 6.4 and defined in more detail in Table 2: M = Malmö, J = Jönköping airport, V = Visby airport, SB = Stockholm-Bromma, Sa = Särna, Su = Sundsvall airport; SV = Storlien-Visjövalen, G = Gunnarn, L = Luleå airport and K = Katterjåkk.*

The discontinuity problem may be avoided by assuming that the simulated grid box values actually are a sample of some continuous physical distribution. A simple and frequently used way of doing this is bilinear interpolation. The continuous field is assumed to coincide with the simulated grid box values at grid box centers ('grid points'), and between these, the field is assumed to be a linear function of both latitude and longitude. The local value thus generally becomes a weighted average of the four nearest GCM simulated grid box values.

Table 2 *Characteristics of the 10 Swedish meteorological stations used in Figs. 6.2 and 6.4. Altitude in HadCM2 is the value obtained by bilinear interpolation of the grid box heights. Station numbers according to Alexandersson et al. (1991).*

Site	Station Number	Latitude	Longitude	Altitude (m)	Altitude in HadCM2
Malmö	5336	55°37'	13°04'	5	20
Visby airport	7840	57°40'	18°20'	42	14
Jönköping Airport	7446	57°45'	14°04'	226	108
Stockholm-Bromma	9720	59°21'	17°57'	7	36
Särna	11341	61°41'	13°09'	435	409
Sundsvall airport	12731	62°31'	17°26'	4	139
Storlien-Visjövalen	13218	63°18'	12°07'	642	399
Gunnarn	14757	64°58'	17°42'	278	341
Luleå airport	16286	65°32'	22°07'	17	108
Katterjåkk	18882	68°25'	18°10'	500	318

Another problem, which cannot be cured by a simple horizontal interpolation, are differences in physiography between GCMs and nature. For example, in mountainous areas there are often substantial small-scale variations in surface topography that are necessarily lacking from a GCM height field. The distributions of land and water also occasionally differ between GCMs and nature, which is in some areas an even more serious problem than differences in orography. For example, as seen from Fig. 6.1, Stockholm and many other towns at the eastern coast of Sweden are actually within sea grid boxes in HadCM2.

One can also try to account for physiographic differences when deriving estimates of local climate from GCM data. But, the various choices associated with physiographical differences and horizontal interpolation make GCM-simulated local climate a somewhat ambiguous concept. In the remainder of this section, we will compare the observed seasonal cycles of surface air temperature and precipitation at Swedish meteorological stations with four alternative interpretations of the HadCM2 control simulation:

1) The HadCM2 simulated temperature or precipitation in the grid box including the station is taken as such.
2) The station value is derived from the four nearest grid box values using bilinear interpolation between grid box centers.
3) As 2), but differences between the (interpolated) HadCM2 surface orography and the actual station height are accounted for. For this purpose, we use the vertical gradients of temperature and precipitation assumed by the CRU data set. For each 100 m in increasing height, surface air temperature is assumed to decrease 0.49-0.60°C and precipitation increase by 3.0-5.5 mm/month. These both vary with season but are (somewhat unrealistically) assumed to be geographically constant in the whole of Europe.

4) As 3), but only land grid boxes are used in the bilinear interpolation (although some meteorological stations are near the coast or on small islands, all of them are over land rather than over water). In this method, the model values for some stations (e.g., Visby, Stockholm, Sundsvall and Luleå) are thus derived from the values at the neighbouring grid boxes only, neglecting the grid box within which the station is actually located.

6.1 Surface air temperature

In Fig. 6.2, the observed seasonal cycles of surface air temperature at the 10 stations indicated in Fig. 6.1 and defined in Table 2 are compared witht the four interpretations of the model-simulated temperature. There are in some cases quite large differences between these four alternatives. As indicated by the definitions above, the difference between methods 2 and 1 arises from bilinear interpolation, that between 3 and 2 from height adjustment, and that between 4 and 3 from rejecting sea grid boxes in the interpolation.

The relative importance of the three choices varies from station to station, but in most cases the height adjustment (method 3 – method 2) is the least important of these. The difference between the actual station height and the bilinearly interpolated HadCM2 orography is below 100 m for six of the ten stations, and for these the height adjustment is thus within about ±0.5°C. The adjustment is in absolute terms largest, roughly -1.3°C, for Storlien-Visjövalen. By contrast, where the gradients in the simulated temperature field are strong and a station is located near a boundary between two grid boxes, the difference due to bilinear interpolation (method 2 – method 1) is frequently considerable. In the most extreme case, bilinear interpolation gives 5°C warmer winter temperatures for Katterjåkk than the nearest grid box value as such. Finally, the differences between methods 4 and 3 are large for most of the ten stations. Rejecting sea grid boxes in the bilinear interpolation regularly lowers the temperature estimate in autumn and in winter, and in most cases raises it in spring and in summer.

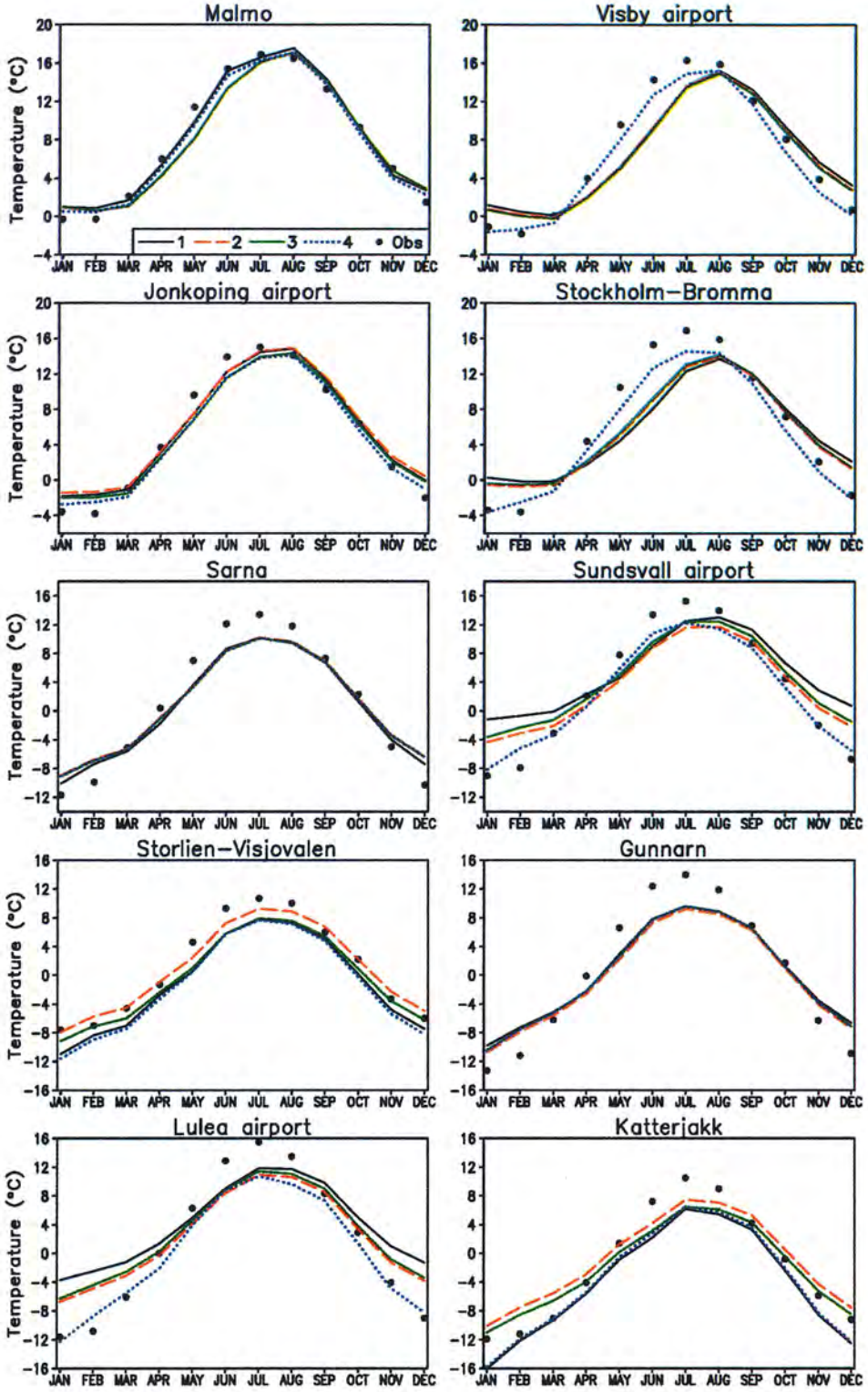

Figure 6.2: *Observed (closed circles) and HadCM2-simulated monthly mean surface air temperatures at 10 Swedish meteorological stations. The four interpretations of the model-simulated local temperature defined in the text are represented with 1 - solid, 2 - long dashed, 3 - short dashed and 4 – dotted lines. Note that the temperature scale differs from station to station.*

There are only two inland stations (Särna and Gunnarn) for which all four methods give very similar temperatures. For both of these, the model gives a too weak annual cycle: simulated temperatures are too warm in winter and too cold in summer. In several other cases, the spread between the different estimates makes the comparison between the modelled and observed station temperatures more problematic. However, regardless of which of the interpretations 1 - 4 is used, the simulated summer temperatures are too cold at all stations, except for Malmö and Jönköping in August. In winter, the model appears to give too warm temperatures for most of the ten stations, but this conclusion is more sensitive to which interpretation method is selected. In particular, for the four stations located within sea grid boxes in HadCM2 (Visby, Stockholm, Sundsvall, Luleå), methods 1-3 all give several degrees to warm winter temperatures but the estimate 4 is close to observations. In addition, as expected, the first three methods give for these stations a markedly delayed seasonal cycle. As an exception to the overall wintertime warmness, all four interpretations of the model simulation give a slightly lower January mean temperature at Storlien-Visjövalen than is observed.

This kind of a comparison was conducted, in a statistical manner, for a total of 477 Swedish stations. In Fig. 6.3, mean and root-mean-square (rms) differences and cross-correlations between the observed and modelled temperatures are shown, again using four different methods to derive the latter. In the averaging, all stations were given the same weight. As the stations are not homogeneously distributed but rather have a somewhat larger density in the densely populated Southern Sweden (about 50% of them are south of 60°N), the statistics might be slightly modified if area-weighted averaging were used.

In terms of the mean difference, methods 1-3 give almost identical results. Although bilinear interpolation and height adjustment may both significantly modify the temperature estimates for individual stations, the resulting positive and negative changes almost average out when a large set of stations is used. These methods all indicate a very substantial cold bias in spring and summer (up to 3.5°C in June) and a warm bias of about 2°C in winter. Method 4 (neglect of sea grid boxes in the interpolation) amplifies, as expected, the seasonal cycle of the model-derived temperatures and thus reduces the cold bias in early summer and, in particular, the warm bias in winter.

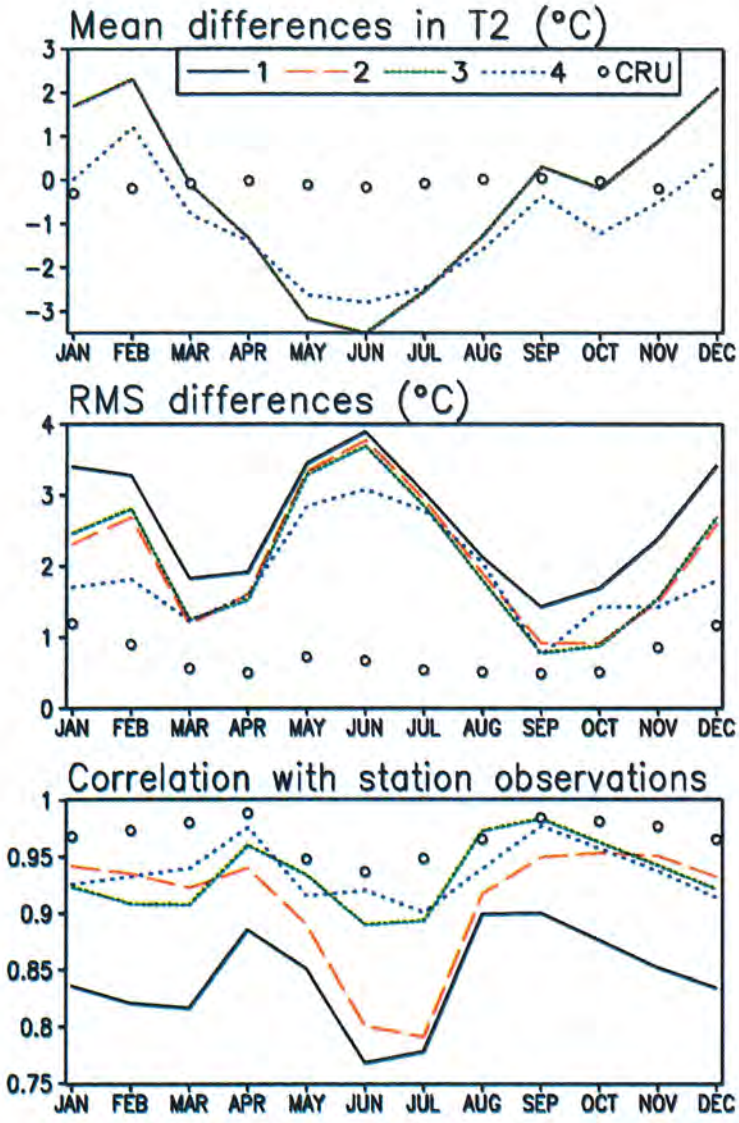

***Figure 6.3**: Mean and root-mean-square differences (°C) and cross-correlations between observed and HadCM2-simulated monthly mean temperatures for 477 Swedish stations. The four lines give the difference or correlation between the four definitions of the model-simulated local temperature (1-solid, 2-long dash, 3 - short dash and 4 - dotted) and station observation; however, the mean differences for 1-3 are too close each other to be resolved separately. Also shown are the differences and correlation between the CRU climatology and station observations (open circles).*

The rms differences between the model and observations are largest in winter and summer, when the mean differences are also largest. Throughout the year, the rms difference to observations is largest when the simulated grid box temperatures are used as such (method 1). Bilinear interpolation (method 2) reduces the rms difference in all months, although only very modestly in summer when the rms difference is dominated by the large overall cold bias. Height adjustment of the simulated temperatures (method 3) also slightly improves the agreement from April to October, but actually worsens it from

from November to March. Finally, the neglect of sea grid boxes in the bilinear interpolation (method 4) reduces the rms errors substantially in midwinter and in late spring and early summer, but increases them slightly in April, August and October.

The cross-correlations between simulated and observed temperatures are by definition independent of the overall biases and are in fact quite high. They are lowest for method 1, but even in this case in most months above 0.8. The increase in correlation given by the height adjustment (method 3 – method 2) is substantial in summer, but is reversed to a slight decrease in winter.

Fig 6.3 also compares the CRU climatology with the actual station observations (to get from the CRU grid to station locations, method 3 with both bilinear interpolation and adjustment of temperature for height differences was used). Differences between the two observational data sets are generally small compared with those between the model simulation and the station observations, but they are not negligible. Although the CRU temperature climatology was derived from station observations, the diurnal means were estimated in a way different from that used by Alexandersson et al. (1991) [Hulme et al. (1995) simply define the mean as the average of daily maximum and minimum], and a smaller number of stations was used. In addition, the 'European mean' vertical lapse rate assumed by the CRU data set (roughly 5°C / km) gives a poor description of true winter conditions in northern Sweden, where the lowest temperatures are in fact observed in valleys rather than on mountain tops (e.g., Raab and Vedin 1995). The too simple form of this height adjustment is also the most obvious explanation to why there is no improvement in winter from method 2 to method 3 in the comparison between HadCM2 and the station observations.

6.2 Precipitation

In Figs. 6.4 and 6.5, a similar comparison is made between HadCM2-simulated and observed precipitation. The same four methods to derive the station value from the model results are used as in the case of temperature.

The comparison for the 10 selected stations (Fig. 6.4) reveals an even more pronounced variation between the four interpretations of the model-simulated precipitation than was the case with temperature. The differences between the nearest grid box value (method 1) and bilinear interpolation (method 2) are for several stations (Särna, Sundsvall, Storlien-Visjövalen, Gunnarn, Katterjåkk) large throughout the year. The impact of the height adjustment (method 3 – method 2) is generally more modest. Finally, when sea grid boxes are neglected in the bilinear interpolation, the estimated summer precipitation increases dramatically at some of the stations located near the Baltic coast (in particular, Visby, Stockholm and Sundsvall). This is due to the fact that HadCM2 simulates much less summer precipitation over the Baltic Sea than over the land areas of Sweden (see Fig. 5.3).

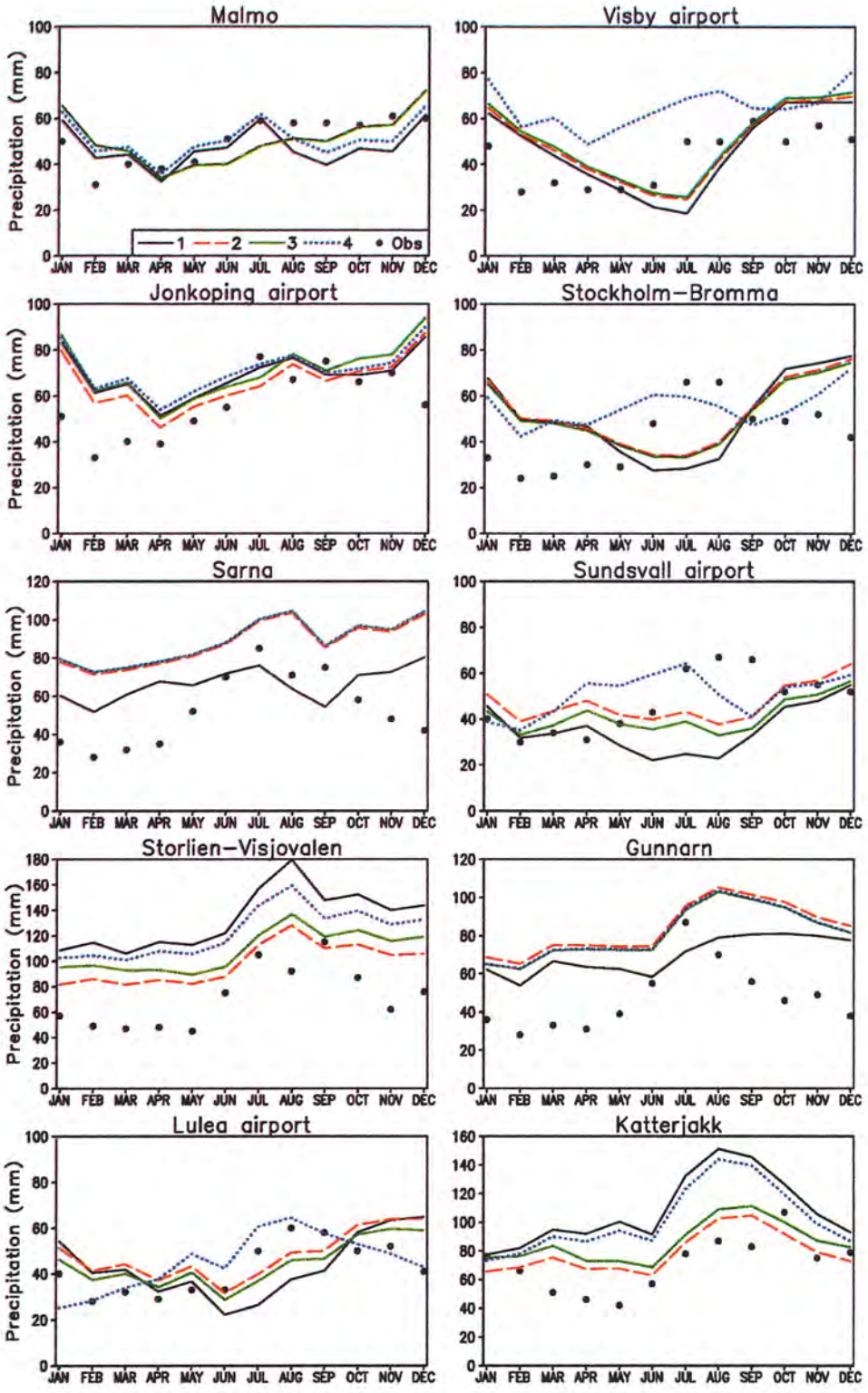

***Figure 6.4**: As Fig. 6.2 but for precipitation (mm/month).*

The total range spanned by the four different interpretations of the model-simulated precipitation is moderately small for only two southern stations, Malmö and Jönköping. In spite of this, all four alternatives clearly exceed the measured values at most stations in winter. At Storlien and Gunnarn, the model simulates much more precipitation than the observations indicate almost throughout the year. On the other hand, the interpretation

methods 1, 2 and 3 all give a clear underestimate of the actual summer precipitation at Visby, Stockholm and Sundsvall.

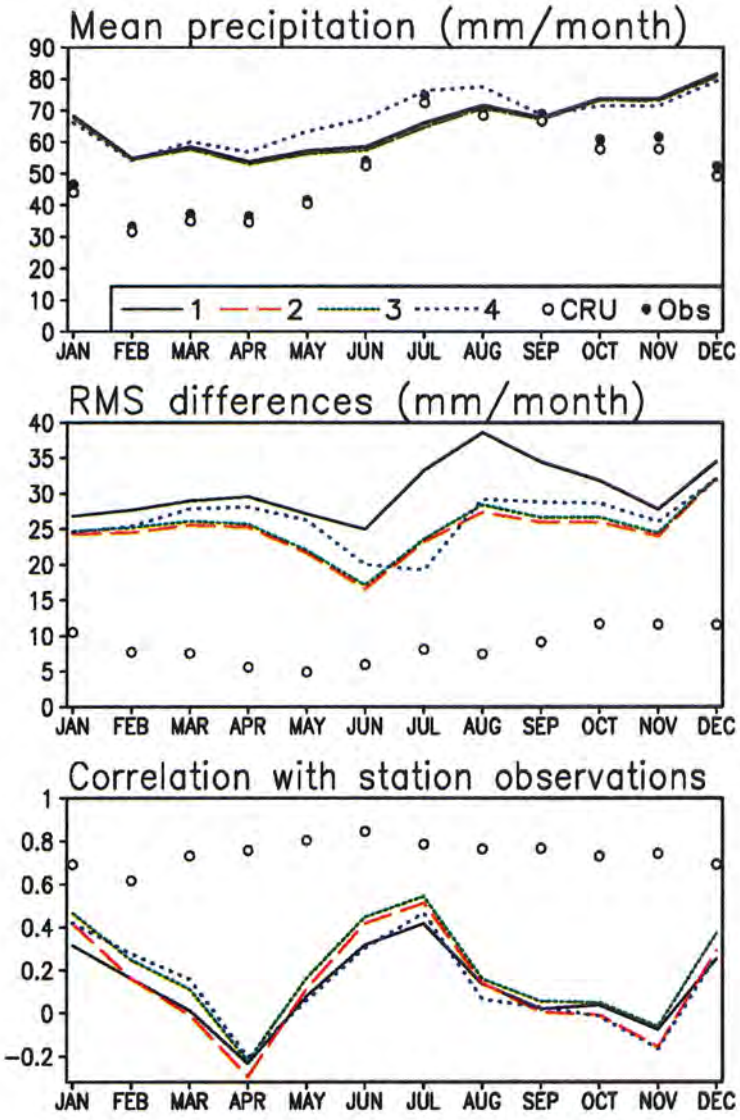

***Figure 6.5**: Comparison between HadCM2-simulated and observed monthly mean precipitation (mm/month) at Swedish precipitation stations. The top panel shows the mean precipitation for 1192 stations derived by using the four interpretations of the HadCM2 simulation (1– solid, 2 – long dash, 3 – short dash and 4 – dotted line), the CRU climatology (open circles) and the actual station observations (closed circles). In the mid- and bottom panels, the rms differences and cross correlations between the other precipitation estimates and the station observations are shown.*

The statistics in Fig. 6.5 include a total of 1192 Swedish precipitation stations. In terms of the all-station mean, methods 1-3 again give very similar results. As could be anticipitated from Fig. 6.4, method 4 yields on the average somewhat more summer precipitation. The model-simulated mean precipitation is in reasonable agreement with observations in summer and early autumn, but larger than observed in late autumn,

winter and spring. However, because there is a dry bias in the observations, the true overestimate in cold season precipitation is not as large as it looks. In terms of the rms differences, method 1 again gives the worst fit with the station observations. The smallest rms differences are generally obtained with method 2 (pure bilinear interpolation) but the highest cross correlations with method 3, which also includes a height adjustment. The improvement in correlation as a result of the height adjustment indicates that the assumed increase in precipitation with increasing height is qualitatively correct, whereas the increase in rms errors may either stem from an error in the magnitude of this increase or be indirectly caused by the biases in the HadCM2 simulation. Overall, the skill of HadCM2 in simulating the distribution of precipitation within Sweden is very limited. All four methods yield somewhat positive (0.3-0.55) cross-correlations with the observations in winter and summer, but the correlations for April and November are in fact slightly negative.

Also shown in Fig. 6.5 is that the precipitation values inferred from the CRU climatology are not identical with the actual station observations. The differences are considerably smaller than those between the model-derived values and the station observations, but still more pronounced than they were in the case of surface air temperature. For example, the cross correlation between the CRU climatology and the stations observations varies from only 0.62 in February to 0.85 in June. The CRU climatology was derived from only a small subset of the stations used in Fig. 6.5, and the adopted height adjustment was very simple. In addition, as only a minority of the 1192 stations were operational during the whole period 1961-1990, some interpolation from nearby stations was frequently needed in deriving the 30-year means (Alexandersson et al., 1991). However, the latter factor seems unimportant, since no improvement in the agreement between the CRU climatology and the station observations was found by restricting the calculation to the stations with no or only a few years of missing data.

7 Interannual variability

The analysis this far has focused on the time mean state of the climate. In this section we complement the picture by studying the interannual variability of surface air temperature and precipitation. In contrast with the discussion in the previous sections, the model-simulated interannual variability is quantified using the 240 years of data in the original control simulation. The 10-year period in the repeated control run is too short for this purpose.

Fig. 7.1 compares the observed and modelled interannual standard deviation of monthly mean surface air temperature in two months, January and July. The estimate for observed variability is derived from the temperature anomaly time series in the CRU data set (Hulme et al. 1995) for 1961-1990.

In January, the model results and the observations are in good agreement, with the exception that the model-simulated interannual variability is somewhat larger in much of Norway. In July, however, the differences between the observed and modelled variability are larger. The observed interannual variability in this month is up to three times smaller than it is in January, but in HadCM2 this seasonal contrast is smaller. The model overestimates the interannual standard deviation of July mean temperature only slightly in northern Finland, Sweden and Norway, but the overestimate grows larger towards south. The standard deviation in the model exceeds the observed one by almost a factor of two in southern Sweden, and locally by a factor of over two in Poland and the former Soviet Union.

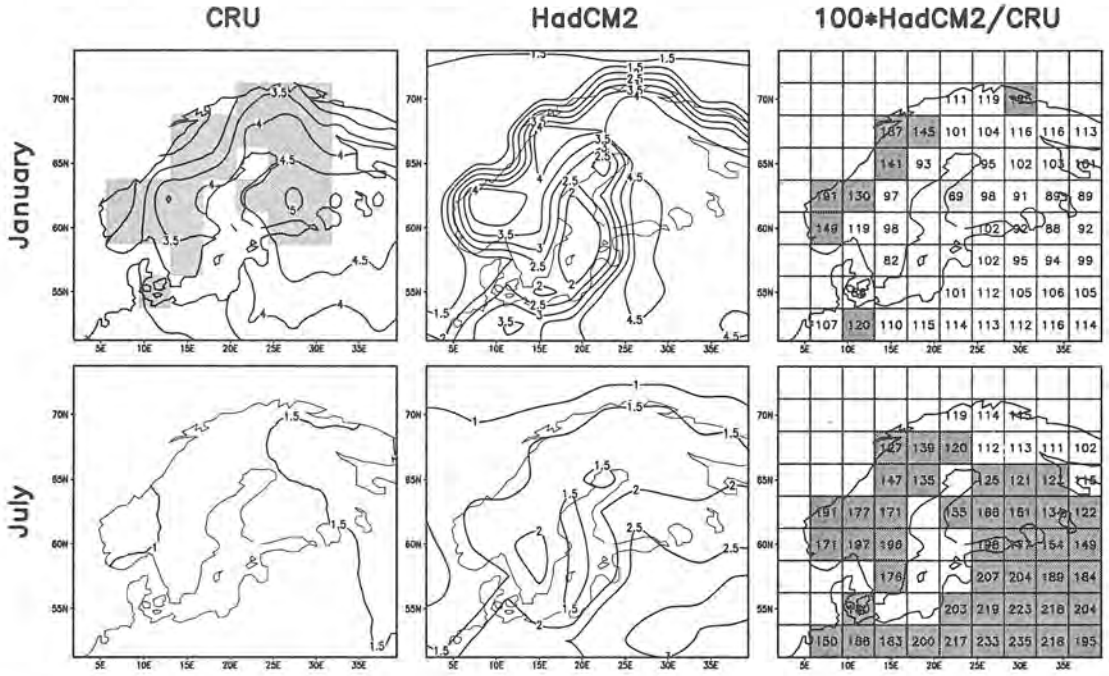

***Figure 7.1**: Interannual standard deviation (°C) of monthly mean surface air temperature in January (above) and July (below). The left panels show the observed standard deviation for 1961-1990 and the midpanels the standard deviation in the HadCM2 control run in 1860-2099. On the right, the ratio between the modelled and observed values is given in per cent. Grid boxes where the modelled standard deviation is over 120% (below 80%) of that observed are marked with dark (light) shading. The shading in the upper left panel shows the Nordic land area used in Figs. 7.2 and 8.4.*

The annual cycles of the observed and modelled interannual standard deviations of monthly mean temperature are further compared in the first panel of Fig. 7.2. Here, area means of the standard deviation are shown for the Nordic land area, defined as the 25 HadCM2 land grid boxes at least partly within the borders of Finland, Sweden, Norway and Denmark (see Fig. 7.1). The modelled standard deviations are shown for the 240-year period as whole and for the 8 non-overlapping 30-year time slices (length of the

observational record) within this period. This gives an idea of the statistical significance of the model-observation differences.

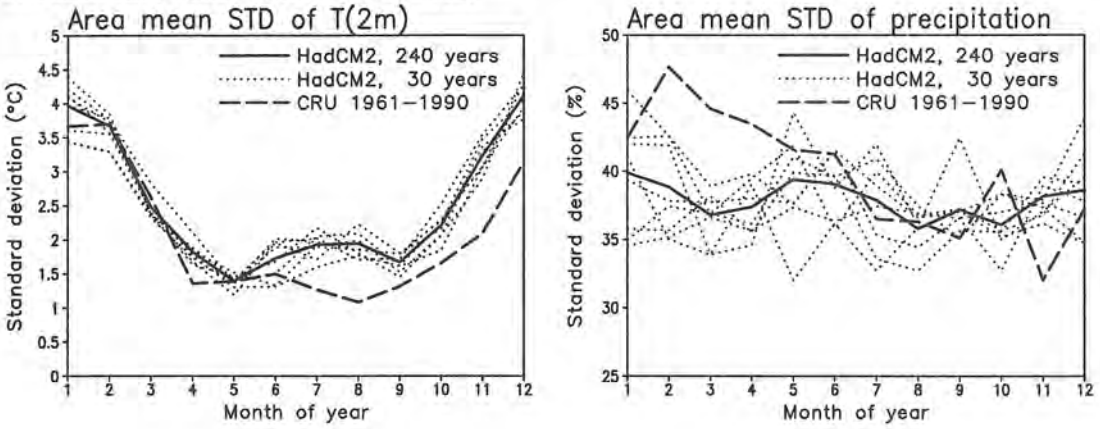

***Figure 7.2**: Nordic land area means of the interannual standard deviation of monthly mean surface air temperature (left) and precipitation (right). The observed standard deviations in 1961-1990 are shown by the dashed line and the standard deviations in HadCM2 in 1860-2099 by the solid line. The eight dotted lines give the standard deviations for the eight non-overlapping 30-year periods in HadCM2. Units: °C for temperature and % of the 30-year/240-year monthly mean for precipitation.*

From January to June excluding April, the observed and modelled standard deviations are close to each other (the observed value is within the spread between the eight individual 30-year periods in the model). In the other months, however, the interannual variability in the model exceeds that in nature. The difference is in relative terms largest in August, when observations indicate a minimum of interannual variability but the model a secondary maximum. This overestimate of interannual variability in summer and autumn becomes even more pronounced towards central and eastern Europe, and it has also been noted by Tett et al. (1997). They attribute it to an excessively strong simulated drying out of soil in summer.

In the second panel of Fig. 7.2, a similar comparison is made for the areally averaged interannual standard deviation of precipitation (expressed as per cent of the long-term monthly mean precipitation in the model or in the observational data set). The modelled 240-year relative standard deviation is in all months between 35 and 40%, which is in good agreement with the observed variability in particular in the latter half of the year. However, the slightly larger observed relative variability in late winter and early spring is not captured by the model. In the finer geographical details, there are naturally larger differerences between the model and the observations than the area means indicate. However, as the differences between the individual 30-year periods in the model simulation are quite large even at the area mean level, a more detailed analysis would probably not be meaningful.

Finally, it is important to note two facts relevant to the interpretation of these results. First, although the CRU data set has a nominal resolution of 0.5° lat x 0.5° lon, the anomaly time series were derived from data sets with a much coarser resolution (5° lat x 5° lon for temperature and 2.5° lat x 3.75° lon for precipitation). This makes, in fact, the comparison of these data with the HadCM2 results more straightforward, but the interannual variability at truly local scales is expected to be larger in particular in the case of precipitation. Second, on the other hand, the observed interannual variability during 1961-1990 may have been to some extent affected by external forcing factors such as anthropogenic changes in the atmospheric composition, changes in solar activity and volcanic eruptions. Therefore, the observational record does not give as pure a realization of internal climate variability as the HadCM2 control simulation.

8 Differences between 10-year and 240-year control climates

With the exception of the previous section, all the analysis in this report has been based on just 10 years of the repeated HadCM2 control simulation. However, in the same manner as in nature, individual decades differ from each other in climate models. In this section we study how representative our 10-year period is of the longer-term behaviour of the HadCM2 model. As the reference we use the 240-year monthly and seasonal means of sea level pressure, surface air temperature and precipitation in the original HadCM2 control simulation. The deviations of the 10-year means from the 240-year means will be here referred to as anomalies.

The seasonal mean anomalies of sea level pressure (Fig. 8.1) are largest in winter, that is, in the season when the interannual variations in general are most pronounced. The anomaly pattern in winter is dominated by a dipole with a low over the North Sea and a high over Russia, and it indicates a southerly or southeasterly anomalous near-surface flow over most of the Nordic Countries In summer, the anomaly field is dominated by a 1.5 hPa high centred in southern Norway. In spring and autumn, the patterns are more diffuse.

The seasonal anomalies of surface air temperature, shown in Fig. 8.2, are mostly quite small. However, a warm anomaly of slightly over 0.5°C occurs in parts of eastern Finland and southern Sweden in winter, and in southernmost Sweden and Denmark in summer. In part of northern Norway in winter, there is conversely a local cold anomaly of slightly over 0.5°C.

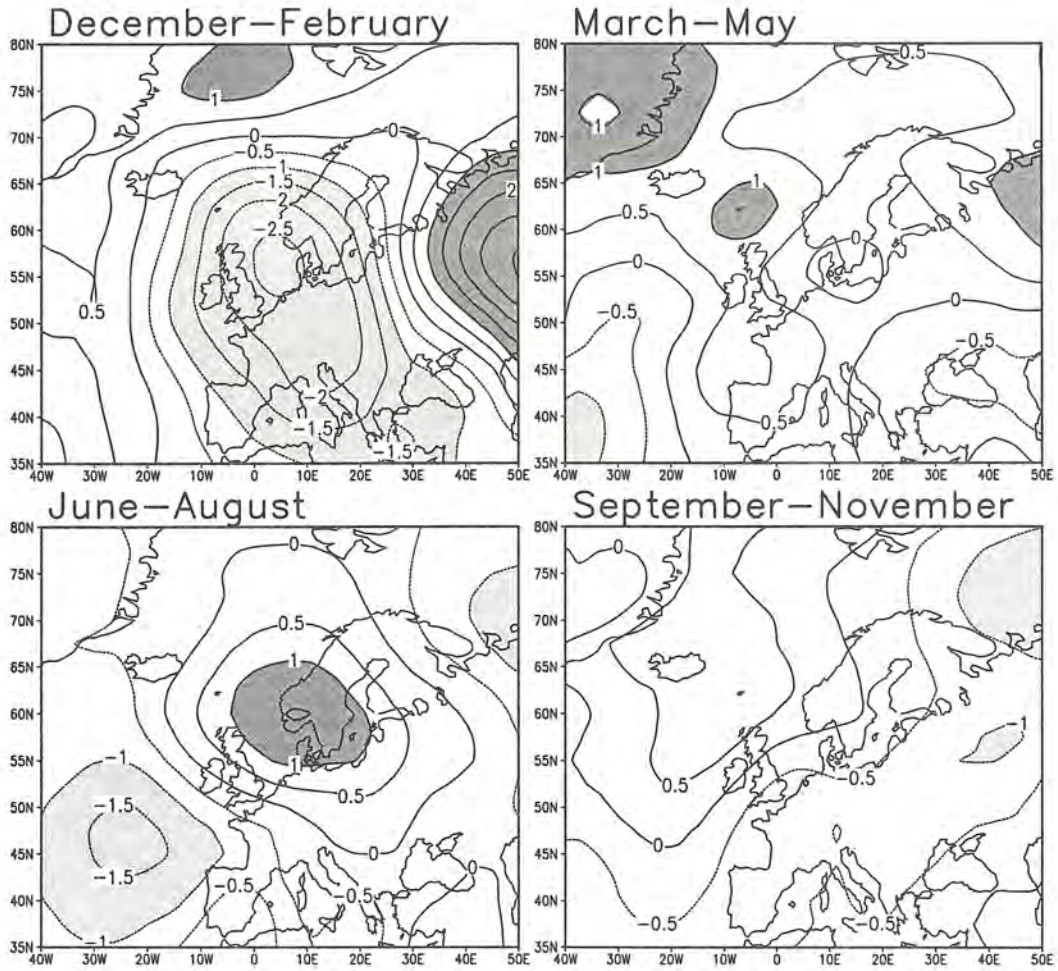

***Figure 8.1**: Seasonal mean anomalies (deviation of the means over 2039-2049 in the repeated control run from the means over 1860-2099 in the original control run) of sea level pressure. Contour interval is 0.5 hPa and anomalies with an absolute value of more than 1 hPa are shaded.*

As averaged over the Nordic land area defined in Fig. 7.1, the seasonal mean temperature anomalies are very small: +0.2°C in winter, -0.1°C in spring, and 0.0°C in summer and autumn. Somewhat larger area mean temperature anomalies occur in some of the individual months. They exceed in absolute value 0.5°C in January (–0.8°C), September (+0.8°C), November (–0.7°C) and December (+0.9°C). The largest local monthly anomalies occur in winter. During 2039-2049, Januaries are up to 2°C colder than average in western Norway, whereas Decembers are up to 2°C colder than average in eastern Finland. Thus, as expected, the magnitude of the anomalies increases towards decreasing temporal (seasonal to monthly) and horizontal (Nordic mean to local) scales.

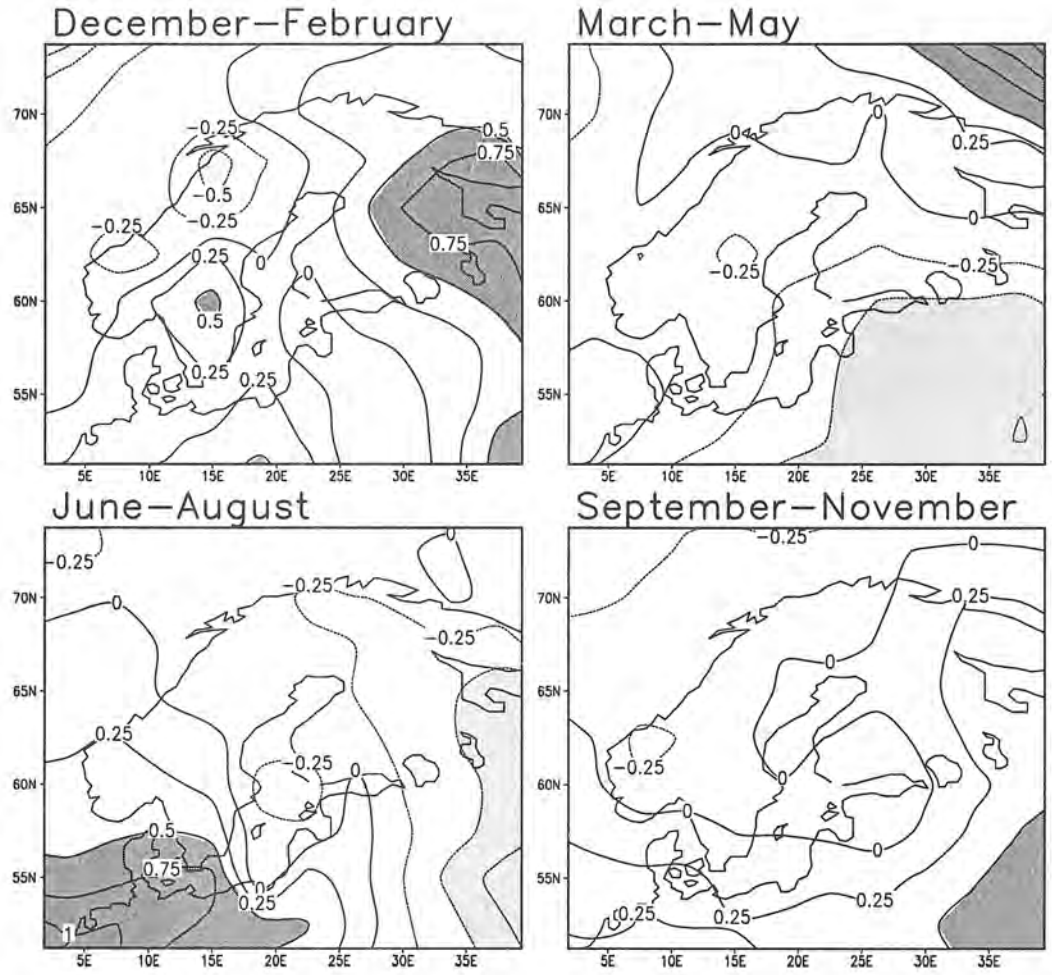

***Figure 8.2**: Seasonal mean anomalies of surface air temperature. Contour interval is 0.25°C and anomalies with an absolute value of more than 0.5°C are shaded.*

As averaged over the Nordic land area defined in Fig. 7.1, the seasonal mean temperature anomalies are very small: +0.2°C in winter, -0.1°C in spring, and 0.0°C in summer and autumn. Somewhat larger area mean temperature anomalies occur in some of the individual months. They exceed in absolute value 0.5°C in January (–0.8°C), September (+0.8°C), November (–0.7°C) and December (+0.9°C). The largest local monthly anomalies occur in winter. During 2039-2049, Januaries are up to 2°C colder than average in western Norway, whereas Decembers are up to 2°C colder than average in eastern Finland. Thus, as expected, the magnitude of the anomalies increases towards decreasing temporal (seasonal to monthly) and horizontal (Nordic mean to local) scales.

Finally, the seasonal anomalies of precipitation are shown in Fig. 8.3. The 10-year mean winter precipitation exceeds the 240-year mean by 5-15% in much of Finland, southern and eastern Sweden and southernmost Norway. On the other hand, a negative precipitation anomaly of up to 20% occurs at the west coast of middle and northern Norway. In summer, there is a substantial (more than 30%) negative anomaly over the southern Baltic Sea and the Baltic states, and a weaker negative anomaly covers much

of Finland, Sweden, Denmark and southern Norway. The precipitation anomalies in spring and autumn are relatively small.

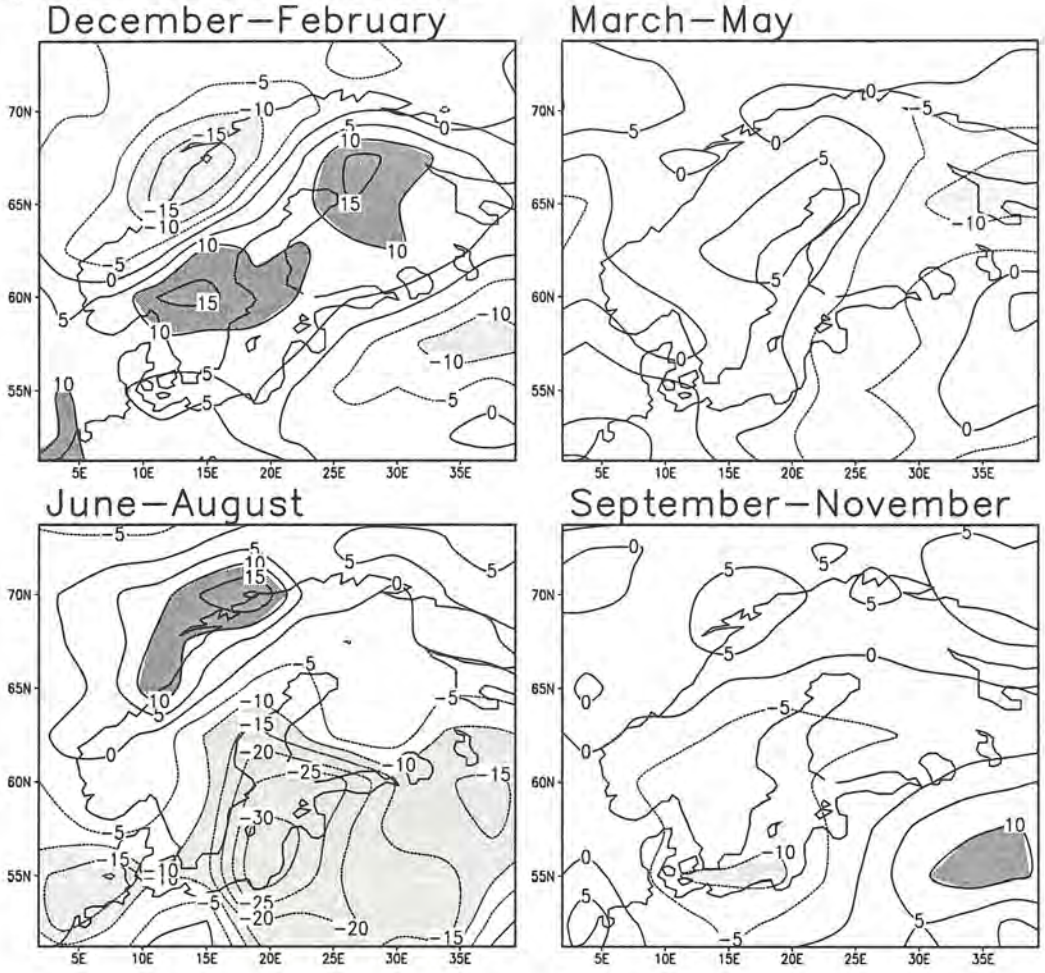

***Figure 8.3**: Seasonal mean anomalies of precipitation, given in per cent of the 240-year mean. Contour interval is 5% and anomalies with an absolute value of more than 10% are shaded.*

As expected, most of the temperature, pressure and precipitation anomalies for 2039-2049 are well within the variability between the individual decades in the original 240-year control run (not shown). In addition, the seasonal anomalies are generally relatively small compared with the differences between the model results and observational estimates discussed in sections 3 and 5. Therefore, the use of 240 years of model data would have only slightly modified the picture of the strengths and the weaknesses of the model that was obtained by using the single decade. Some aspects of the 240-year climate are slightly closer to observations than the same aspects of the 10-year climate, some others actually further away. As an example of the former, the 240-year period shows a somewhat larger summer-winter contrast in precipitation in most of Sweden and a less severe underestimate of summer precipitation in the Baltic States (compare Figs. 7.1 and 5.3). In any case, some of the anomalies in the 10-year climate are large

enough to be kept in mind when comparing the HadCM2 control run with the run with increased CO_2 or when interpreting dynamical and statistical downscaling experiments based on these global model simulations.

A significant part of the interannual and interdecadal variations in the climate of Northern Europe in particular in winter are associated with the North Atlantic Oscilllation (NAO; e.g., Hurrel and Van Loon, 1997). The NAO is basically an irregular variation in the mean pressure gradient between the Icelandic low and the Atlantic subtropical high. During positive phases of the oscillation, the wintertime mean Icelandic low is deep and the Azores high strong, and strong westerly winds bring relatively warm air from the Atlantic to northern Europe. When, in contrast, NAO is in its negative phase, the Icelandic low and the Azores high are both weaker than average, and lack of warm advection from the Atlantic usually leads to below-average winter temperatures in northern Europe. The fundamental causes (internal atmospheric variation or partly forced by SST anomalies and/or changes in atmospheric composition) and nature (is there statistically significant interannual autocorrelation or not) of the phenomenon are still discussed (e.g., Appenzeller et al. 1998, Graf et al. 1998, Sutton and Allen 1997).

The interannual variability of NAO in the HadCM2 control simulation is illusrated in Fig. 8.4. The index of oscillation was derived from the December-February mean pressure difference between the grid box closest to Lisbon, Portugal (7.5°W, 40°N) and the grid box closest to Akureyri, Iceland (22.5°E, 65°N). This pressure difference was normalized by subtracting the 240-year (1860-2099) mean wintertime pressure difference in the original control run and by dividing by the corresponding interannual standard deviation.

For comparison, the NAO index time series for winters 2039-2040 through 2048-2049 is shown for both the repeated control run used at the Rossby Centre and for the original control run. The two runs are indeed far from identical, and in this respect it actually is the repeated run in which the 10-year period closer to the normal. The 10-winter mean NAO index in the repeated control run is just slightly negative (-0.19). As seen from Fig. 8.1, the pressure anomalies in Iceland and Portugal are both small. There is, as expected, some interannual variation, but neither the negative nor the positive phase of NAO is dominating strongly. In the same decade in the original control run, by contrast, there are several winters with strongly negative NAO index but only two winters with a slightly positive index. The 10-winter NAO index for this run is –0.82.

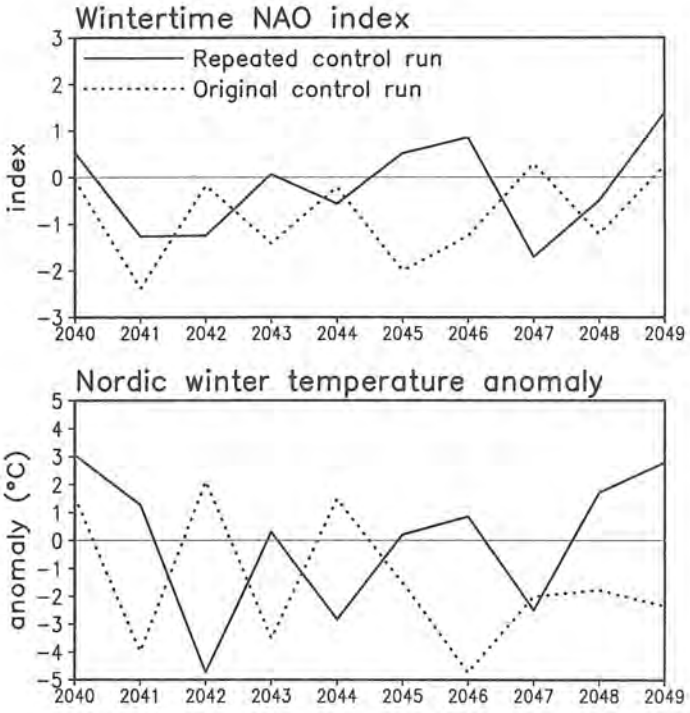

***Figure 8.4**: Interannual wintertime variations of the North Atlantic Oscillation index (above) and the Nordic land area mean temperature anomaly (below) in the repeated (solid) and in the original HadCM2 control run (dotted). A winter begins from the beginning of December preceding the year given on the x-axis and extends to the end of February.*

In the lower part of Fig. 8.4, the anomalies of the Nordic mean December-February surface air temperature relative to the 240-year mean are shown. In both the original and the repeated control run, most of the winters with positive (negative) NAO index are warmer (colder) than the average. In the 240-year run, the correlation between the interannual variations of the NAO index and this area mean temperature is 0.56. Consistent with the dominantly negative phase of NAO during this 10-year period in the original control run, the 10-winter mean temperature anomaly in this run is markedly negative, -1.5°C. By contrast, as already mentioned, the corresponding temperature anomaly in the repeated control run is very small.

9 Summary

This report has studied some aspects of the ability of the HadCM2 ocean-atmosphere general circulation model in simulating the present climate in Northern Europe. The fundamental motivation for studying this issue is the use of HadCM2 in the dynamical and statistical downscaling work being done within the SWEdish regional CLImate Modelling programme SWECLIM. Investigating the large-scale climate simulated by HadCM2 gives an indication on how good input data the model gives for these regional downscaling techniques. Comparison of the simulated and observed climates at the

regional and local scales provides, in turn, a benchmark needed in estimating the actual value of these dowscaling techniques.

The main focus of the analysis has been a rerun 10-year period, 2039-2049, of the HadCM2 control run (here referred to as the repeated control run), which provides the boundary conditions for the first SWECLIM dynamical downscaling experiment. Analysis of the atmospheric circulation around Northern Europe reveals good overall agreement with observational data, but also some quantitative deficiencies. Two of the more notable include

- Slightly too southerly wintertime Icelandic low having a too weak northeastward extension towards the Arctic Ocean. This deficiency in the time-mean pressure field implies a weaker than observed time mean southwesterly flow over Scandinavia in winter.
- A general cold bias of a few °C in lower tropospheric temperatures in Northern Europe in summer.

The model-simulated time mean surface climate over the Nordic Countries was compared with the CRU climatology (Hulme et al. 1995). Focusing once again on the differences rather than on the similarities between the model results and the observed climate, we found that

- HadCM2 underestimates the average surface air temperature over the Nordic countries by 2-4°C in summer, and by a slightly smaller amount in spring and in most of the area in autumn. In winter, a local warm bias occurs in a few gridboxes surrounding the Baltic Sea, which unrealistically lacks ice cover in the model even in cold winters.
- The sharp but narrow observed maximum of precipitation at the western slope of the Norwegian mountains is in the model weaker, broader, and further east. In the rest of the Nordic area, the simulated precipitation systematically exceeds the measured amounts in particular in winter and spring, although this is partly explained by a dry bias in the measurements.
- Simulated total cloudiness is generally higher (typically by 10% of full cover) than observations indicate.

After the grid-scale comparison, the model-simulated temperatures and precipitation were compared with data from individual Swedish meteorological stations. A major complication, and ambiguity, in such local-scale comparison is the derivation of the station values from the grid box values simulated by the model. Bilinear interpolation of the grid box values to the station locations was found to yield a general improvement in the verification statistics over simply using the nearest grid box value as such. However, the improvement resulting from the adjustment of the simulated values for the orographic differences between the model and the real world was not systematic. This

may be so either because the adjustments applied were not optimal for Swedish conditions, or because the potential benefit of the adjustments was masked by larger-scale biases in the simulated climate. Similarly, a crude way for accounting for the differences in the land-sea distribution between the model and nature (the neglect of sea grid boxes in bilinear interpolation) improved the agreement in some but by no means all cases.

Most of this report focused on the temporally averaged climate, in part because 10 years of data forms a rather limited sample for quantifying the simulated variability. By using the 240-year long original control run, the interannual variability of monthly mean temperature and precipitation in northern Europe could nevertheless be studied. The largest difference to observed grid-scale climate was a general overestimate of interannual temperature variability in summer and autumn, in particular in the southern parts of the area.

The original 240-year control run was also used to study how representative the 10-year repeated control run is from the longer-term climate of the model. As a general rule, the differences between the 10-year and 240-year means were significantly smaller than the biases of the former relative to observational data. Still, some of these differences are certainly large enough to be of concern when comparing the 10-year control run with a similar run with increased CO_2. As expected, the differences between the 10-year and 240-year means generally increase towards smaller spatial (the whole Nordic area → individual grid boxes) and temporal (annual → seasonal → monthly means) scales.

Acknowledgements

The HadCM2 model data used for this study were provided by the Hadley Centre and the U. K. Meteorological Office. Part of these data were obtained via the Climate Impacts LINK Project (Department of Environment Contract EPG 1/1/16), which also provided the CRU gridded surface climatology for 1961-1990. Also acknowledged are Hans Alexandersson for processing the Swedish station observations, and Colin Jones and Markku Rummukainen for their comments on the draft versions of this report. This work is part of the SWECLIM programme, funded by MISTRA and SMHI.

References

Alexandersson, H., C. Karlström, and S. Larsson-McCann, 1991: Temperature and precipitation in Sweden 1961-1990. Reference normals. SMHI Meteorologi nr 81, Norrköping, Sweden, 88 pp. (in Swedish).

Appenzeller, C., T. F. Stocker, and M. Anklin, 1998: North Atlantic Oscillation dynamics recorded in Greenland ice cores. *Science*, **282**, 446-449.

Cullen, M. J. P., and Davies, T., 1991: A conservative split explicit integration scheme with fourth order horizontal advection. *Quart. J. Roy. Meteor. Soc.*, **117**, 993-1002.

Giorgi, F., and L. O. Mearns, 1991: Approaches to the simulation of regional climate change: a review. *Rev. Geophys.*, **29**, 191-216.

Graf, H.-F., I. Kirchner, and J. Perlwitz, 1998: Changing lower stratospheric circulation: the role of ozone and greenhouse gases. *J. Geophys. Res.*, **103**, 11251-11261.

Gregory, D., and S. Allen, 1991: The effect of convective scale downdraughts upon NWP and climate model simulations. 9th Conf Numerical Weather Prediction, Denver, CO, Am. Meteorol. Soc., 122-123.

Gregory, D., and P. R. Rowntree, 1990: A mass flux convection scheme with representation of ensemble characteristics and stability dependent closure. *Mon. Wea. Rev.*, **118**, 1483-1506.

Hoskins, B. J., H. H. Hsu, I. N. James, M. Masutani, P. D. Sardesmukh, and G. H. White, 1989: Diagnostics of the global atmospheric circulation based on ECMWF analyses 1979-1989. WCRP Rep. 27, 217 pp. [available from WMO/WCRP, 41 Avenue Giuseppe-Motta, 1211 Geneva 2, Switzerland].

Houghton, J. T., L. G. Meira Filho, B. A. Callander, N. Harris, A. Kattenberg, and K. Maskell, Eds., 1996: *Climate Change 1995. The Science of Climate Change.* Cambridge University Press, 572 pp.

Hulme, M., D. Conway, P. D. Jones, T. Jiang, X. Zhou, E. M. Barrow and C. Turney, 1995: A 1961-90 gridded surface climatology for Europe. A report accompanying the dataset available through the Climate Impacts LINK Project. Climatic Research Unit, University of East Anglia, Norwich, UK, 50 pp.

Hurrel, J. W. and H. van Loon, 1997: Decadal variations in climate associated with the North Atlantic Oscillation. *Clim. Change*, **36**, 301-326.

Johns, T. C., 1996: A Description of the Second Hadley Centre Coupled Model (HADCM2). Hadley Centre for Climate Prediction and Research Rep. 71, 26 pp. [availabie from Hadley Centre, Meteorological Office, London Road, Bracknell, Berkshire RG12 2SY, United Kingdom].

Johns, T.C., R. E. Carnell, J. F. Crossley, J. M. Gregory, J. F. B. Mitchell, C. A. Senior, S. F. B. Tett, and R. A. Wood, 1997: The second Hadley Centre coupled atmosphere-ocean GCM: Model description, spinup and validation. *Climate Dyn.*, **13**, 103-134.

Legates, D. R., and C. J. Willmott, 1990: Mean seasonal and spatial variability in gauge-corrected, global precipitation. *Int. J. Climatol.*, **10**, 111-127.

Levitus S., and T. P. Boyer, 1994: World Ocean Atlas 1994. Volume 4: Temperature. NOAA ATLAS NESDIS 4, 117 pp.

Mesinger, F., 1981: Horizontal advection schemes on a staggered grid, an enstrophy and energy conserving model. *Mon. Wea. Rev.*, **109**, 467-478.

Raab, B., and H. Vedin, Eds., 1995: Climate, Lakes and Rivers. National Atlas of Sweden, vol 14, 176 pp.

Rossow, W. B., A. W. Walker, D. E. Beuschel, and M. D. Roiter, 1996: International satellite cloud climatology project (ISCCP): Documentation of new cloud data sets. WMO/TD-No. 737, 115 pp. [available from World Meteorological Organization, 41 Avenue Giuseppe Motta, 1211 Geneva 2, Switzerland].

Räisänen, J., 1997: Climate response to increasing CO_2 and anthropogenic sulphate aerosols – comparison between two models. Report No. 46, Department of Meteorology, University of Helsinki, 80 pp.

Santer, B. D., T. M. L. Wigley, T. P. Barnett, and E. Anyamba, 1996: Detection of climate change and attribution of causes. *Climate Change 1995. The Science of Climate Change*, J. T. Houghton, L. G. Meira Filho, B. A. Callander, N. Harris, A. Kattenberg, and K. Maskell, Eds., Cambridge University Press, 407-443.

Slingo, A., 1989: A GCM parameterization for the shortwave radiative properties of water clouds. *J. Atmos. Sci*, **46**, 1419-1427.

Slingo, A., and R. C. Wilderspin, 1986: Development of a revised longwave radiation scheme for an atmospheric general circulation model. *Quart. J. Roy. Meteor. Soc.*, **112**, 371-386.

Sutton, R. T., and M. R. Allen, 1997: Decadal predictability of North Atlantic sea surface temperature and climate. *Nature*, **388**, 563-565.

Smith, R. N. B., 1990: A scheme for predicting layer clouds and their water content in a general circulation model. *Quart. J. Roy. Meteor. Soc.*, **116**, 435-460.

Tett, S. F. B., T. C. Johns, and J. F. B. Mitchell, 1997: Global and regional variability in a coupled AOGCM. Climate Dyn., 13, 303-323.

Warrilow, D. A., A. B. Sangster, and A. Slingo, 1986: Modelling of land surface processes and their influence on European climate. Met O 20 Dynamical Climatology Technical Note 38, Meteorological Office, Bracknell, UK.

SMHIs publications

SMHI publishes six report series. Three of these, the R-series, are intended for international readers and are in most cases written in English. For the others the Swedish language is used.

Names of the Series	**Published since**
RMK (Report Meteorology and Climatology)	1974
RH (Report Hydrology)	1990
RO (Report Oceanography)	1986
METEOROLOGI	1985
HYDROLOGI	1985
OCEANOGRAFI	1985

Earlier issues published in serie RMK

1 Thompson, T., Udin, I., and Omstedt, A. (1974)
Sea surface temperatures in waters surrounding Sweden.

2 Bodin, S. (1974)
Development on an unsteady atmospheric boundary layer model.

3 Moen, L. (1975)
A multi-level quasi-geostrophic model for short range weather predictions.

4 Holmström, I. (1976)
Optimization of atmospheric models.

5 Collins, W.G. (1976)
A parameterization model for calculation of vertical fluxes of momentum due to terrain induced gravity waves.

6 Nyberg, A. (1976)
On transport of sulphur over the North Atlantic.

7 Lundqvist, J.-E., and Udin, I. (1977)
Ice accretion on ships with special emphasis on Baltic conditions.

8 Eriksson, B. (1977)
Den dagliga och årliga variationen av temperatur, fuktighet och vindhastighet vid några orter i Sverige.

9 Holmström, I., and Stokes, J. (1978)
Statistical forecasting of sea level changes in the Baltic.

10 Omstedt, A., and Sahlberg, J. (1978)
Some results from a joint Swedish-Finnish sea ice experiment, March, 1977.

11 Haag, T. (1978)
Byggnadsindustrins väderberoende, seminarieuppsats i företagsekonomi, B-nivå.

12 Eriksson, B. (1978)
Vegetationsperioden i Sverige beräknad från temperaturobservationer.

13 Bodin, S. (1979)
En numerisk prognosmodell för det atmosfäriska gränsskiktet, grundad på den turbulenta energiekvationen.

14 Eriksson, B. (1979)
Temperaturfluktuationer under senaste 100 åren.

15 Udin, I., och Mattisson, I. (1979)
Havsis- och snöinformation ur datorbearbetade satellitdata - en modellstudie.

16 Eriksson, B. (1979)
Statistisk analys av nederbördsdata. Del I. Arealnederbörd.

17 Eriksson, B. (1980)
Statistisk analys av nederbördsdata. Del II. Frekvensanalys av månadsnederbörd.

18 Eriksson, B. (1980)
Årsmedelvärden (1931-60) av nederbörd, avdunstning och avrinning.

19 Omstedt, A. (1980)
A sensitivity analysis of steady, free floating ice.

20 Persson, C., och Omstedt, G. (1980)
En modell för beräkning av luftföroreningars spridning och deposition på mesoskala.

21 Jansson, D. (1980)
Studier av temperaturinversioner och vertikal vindskjuvning vid Sundsvall-Härnösands flygplats.

22 Sahlberg, J., and Törnevik, H. (1980)
A study of large scale cooling in the Bay of Bothnia.

23 Ericson, K., and Hårsmar, P.-O. (1980)
Boundary layer measurements at Klock-rike. Oct. 1977.

24 Bringfelt, B. (1980)
A comparison of forest evapotranspiration determined by some independent methods.

25 Bodin, S., and Fredriksson, U. (1980)
Uncertainty in wind forecasting for wind power networks.

26 Eriksson, B. (1980)
Graddagsstatistik för Sverige.

27 Eriksson, B.(1981)
Statistisk analys av nederbördsdata. Del III. 200-åriga nederbördsserier.

28 Eriksson, B. (1981)
Den "potentiella" evapotranspirationen i Sverige.

29 Pershagen, H. (1981)
Maximisnödjup i Sverige (perioden 1905-70).

30 Lönnqvist, O. (1981)
Nederbördsstatistik med praktiska tillämpningar.
(Precipitation statistics with practical applications.)

31 Melgarejo, J.W. (1981)
Similarity theory and resistance laws for the atmospheric boundary layer.

32 Liljas, E. (1981)
Analys av moln och nederbörd genom automatisk klassning av AVHRR-data.

33 Ericson, K. (1982)
Atmospheric boundary layer field experiment in Sweden 1980, GOTEX II, part I.

34 Schoeffler, P. (1982)
Dissipation, dispersion and stability of numerical schemes for advection and diffusion.

35 Undén, P. (1982)
The Swedish Limited Area Model. Part A. Formulation.

36 Bringfelt, B. (1982)
A forest evapotranspiration model using synoptic data.

37 Omstedt, G. (1982)
Spridning av luftförorening från skorsten i konvektiva gränsskikt.

38 Törnevik, H. (1982)
An aerobiological model for operational forecasts of pollen concentration in the air.

39 Eriksson, B. (1982)
Data rörande Sveriges temperaturklimat.

40 Omstedt, G. (1984)
An operational air pollution model using routine meteorological data.

41 Persson, C., and Funkquist, L. (1984)
Local scale plume model for nitrogen oxides. Model description.

42 Gollvik, S. (1984)
Estimation of orographic precipitation by dynamical interpretation of synoptic model data.

43 Lönnqvist, O. (1984)
Congression - A fast regression technique with a great number of functions of all predictors.

44 Laurin, S. (1984)
Population exposure to SO and NO_x from different sources in Stockholm.

45 Svensson, J. (1985)
Remote sensing of atmospheric tempera-ture profiles by TIROS Operational Vertical Sounder.

46 Eriksson, B. (1986)
Nederbörds- och humiditetsklimat i Sverige under vegetationsperioden.

47 Taesler, R. (1986)
Köldperioden av olika längd och förekomst.

48 Wu Zengmao (1986)
Numerical study of lake-land breeze over Lake Vättern, Sweden.

49 Wu Zengmao (1986)
Numerical analysis of initialization procedure in a two-dimensional lake breeze model.

50 Persson, C. (1986)
Local scale plume model for nitrogen oxides. Verification.

51 Melgarejo, J.W. (1986)
An analytical model of the boundary layer above sloping terrain with an application to observations in Antarctica.

52 Bringfelt, B. (1986)
Test of a forest evapotranspiration model.

53 Josefsson, W. (1986)
Solar ultraviolet radiation in Sweden.

54 Dahlström, B. (1986)
Determination of areal precipitation for the Baltic Sea.

55 Persson, C. (SMHI), Rodhe, H. (MISU), De Geer, L.-E. (FOA) (1986)
The Chernobyl accident - A meteorological analysis of how radionucleides reached Sweden.

56 Persson, C., Robertson, L. (SMHI), Grennfelt, P., Kindbom, K., Lövblad, G., och Svanberg, P.-A. (IVL) (1987)
Luftföroreningsepisoden över södra Sverige 2 - 4 februari 1987.

57 Omstedt, G. (1988)
An operational air pollution model.

58 Alexandersson, H., Eriksson, B. (1989)
Climate fluctuations in Sweden 1860 - 1987.

59 Eriksson, B. (1989)
Snödjupsförhållanden i Sverige - Säsongerna 1950/51 - 1979/80.

60 Omstedt, G., Szegö, J. (1990)
Människors exponering för luftföroreningar.

61 Mueller, L., Robertson, L., Andersson, E., Gustafsson, N. (1990)
Meso-γ scale objective analysis of near surface temperature, humidity and wind, and its application in air pollution modelling.

62 Andersson, T., Mattisson, I. (1991)
A field test of thermometer screens.

63 Alexandersson, H., Gollvik, S., Meuller, L. (1991)
An energy balance model for prediction of surface temperatures.

64 Alexandersson, H., Dahlström, B. (1992)
Future climate in the Nordic region - survey and synthesis for the next century.

65 Persson, C., Langner, J., Robertson, L. (1994)
Regional spridningsmodell för Göteborgs och Bohus, Hallands och Älvsborgs län. (A mesoscale air pollution dispersion model for the Swedish west-coast region. In Swedish with captions also in English.)

66 Karlsson, K.-G. (1994)
Satellite-estimated cloudiness from NOAA AVHRR data in the Nordic area during 1993.

67 Karlsson, K-G. (1996)
Cloud classifications with the SCANDIA model.

68 Persson, C., Ullerstig, A. (1996)
Model calculations of dispersion of lindane over Europe. Pilot study with comparisons to measurements around the Baltic Sea and the Kattegat.

69 Langner, J., Persson, C., Robertson, L., and Ullerstig, A. (1996)
Air pollution Assessment Study Using the MATCH Modelling System. Application to sulfur and nitrogen compounds over Sweden 1994.

70 Robertson, L., Langner, J., Engardt, M. (1996)
MATCH - Meso-scale Atmosperic Transport and Chemistry modelling system.

71 Josefsson, W. (1996)
Five years of solar UV-radiation monitoring in Sweden.

72 Persson, C., Ullerstig, A., Robertson, L., Kindbom, K., Sjöberg, K. (1996)
The Swedish Precipitation Chemistry Network. Studies in network design using the MATCH modelling system and statistical methods.

73 Robertson, L. (1996)
Modelling of anthropogenic sulfur deposition to the African and South American continents.

74 Josefsson, W. (1996)
Solar UV-radiation monitoring 1996.

75 Häggmark, L., Ivarsson, K.-I. (SMHI), Olofsson, P.-O. (Militära vädertjänsten). (1997)
MESAN - Mesoskalig analys.

76 Bringfelt, B, Backström, H, Kindell, S, Omstedt, G, Persson, C, Ullerstig, A. (1997)
Calculations of PM-10 concentrations in Swedish cities- Modelling of inhalable particles

77 Gollvik, S. (1997)
The Teleflood project, estimation of precipitation over drainage basins.

78 Persson, C., Ullerstig, A. (1997)
Regional luftmiljöanalys för Västmanlands län baserad på MATCH modell-beräkningar och mätdata - Analys av 1994 års data

79 Josefsson, W., Karlsson, J.-E. (1997)
Measurements of total ozone 1994-1996.

80 Rummukainen, M. (1997)
Methods for statistical downscaling of GCM simulations.

81 Persson, T. (1997)
Solar irradiance modelling using satellite retrieved cloudiness - A pilot study

82 Langner, J., Bergström, R. (SMHI) and Pleijel, K. (IVL) (1998)
European scale modelling of sulfur, oxidized nitrogen and photochemical oxidants. Model development and evaluation for the 1994 growing season.

83 Rummukainen, M., Räisänen, J., Ullerstig, A., Bringfelt, B., Hansson, U., Graham, P., Willén, U. (1998)
RCA - Rossby Centre regional Atmospheric climate model: model description and results from the first multi-year simulation.

SMHI
Swedish Meteorological and Hydrological Institute
SE 601 76 Norrköping, Sweden.
Tel +46 11-495 80 00. Fax +46 11-495 80 01

ISSN 0347-2116